Free Radical Biology and Medicine 222 (2024) 607–624

Contents lists available at ScienceDirect

Free Radical Biology and Medicine

journal homepage: www.elsevier.com/locate/freeradbiomed

Activation of macroautophagy and chaperone-mediated autophagy in human skeletal muscle by high-intensity exercise in normoxia and hypoxia and after recovery with or without post-exercise ischemia

Miriam Martinez-Canton [a,b], Victor Galvan-Alvarez [a,b], Angel Gallego-Selles [a,b], Miriam Gelabert-Rebato [a,b], Eduardo Garcia-Gonzalez [a,b], Juan Jose Gonzalez-Henriquez [b,c], Marcos Martin-Rincon [a,b,1], Jose A.L. Calbet [a,b,d,1,*]

[a] Department of Physical Education, University of Las Palmas de Gran Canaria, Campus Universitario de Tafira s/n, Las Palmas de Gran Canaria, 35017, Spain
[b] Research Institute of Biomedical and Health Sciences (IUIBS), University of Las Palmas de Gran Canaria, Canary Islands, Spain
[c] Department of Mathematics, University of Las Palmas de Gran Canaria, Campus Universitario de Tafira s/n, Las Palmas de Gran Canaria, 35017, Spain
[d] Department of Physical Performance, Norwegian School of Sport Sciences, Oslo, Norway

ARTICLE INFO

Keywords:
Autophagy
Biopsies
Exercise
Fatigue
Hypoxia
Ischemia
Signaling

ABSTRACT

Autophagy is essential for the adaptive response to exercise and physiological skeletal muscle functionality. However, the mechanisms leading to the activation of macroautophagy and chaperone-mediated autophagy in human skeletal muscle in response to high-intensity exercise remain elusive. Our findings demonstrate that macroautophagy and chaperone-mediated autophagy are stimulated by high-intensity exercise in normoxia (P_IO_2: 143 mmHg) and severe acute hypoxia (P_IO_2: 73 mmHg) in healthy humans. High-intensity exercise induces macroautophagy initiation through AMPKα phosphorylation, which phosphorylates and activates ULK1. ULK1 phosphorylates BECN1 at Ser^{15}, eliciting the dissociation of BECN1-BCL2 crucial for phagophore formation. Besides, high-intensity exercise elevates the LC3B-II:LC3B–I ratio, reduces total SQSTM1/p62 levels, and induces *p*-Ser^{349} SQSTM1/p62 phosphorylation, suggesting heightened autophagosome degradation. PHAF1/MYTHO, a novel macroautophagy biomarker, is highly upregulated in response to high-intensity exercise. The latter is accompanied by elevated LAMP2A expression, indicating chaperone-mediated autophagy activation regardless of post-exercise HSPA8/HSC70 downregulation. Despite increased glycolytic metabolism, severe acute hypoxia does not exacerbate the autophagy signaling response. Signaling changes revert within 1 min of recovery with free circulation, while the application of immediate post-exercise ischemia impedes recovery. Our study concludes that macroautophagy and chaperone-mediated autophagy pathways are strongly activated by high-intensity exercise, regardless of PO_2, and that oxygenation is necessary to revert these signals to pre-exercise values. PHAF1/MYTHO emerges as a pivotal exercise-responsive autophagy marker positively associated with the LC3B-II:LC3B–I ratio.

1. Introduction

Human skeletal muscle (hSKM), which accounts for approximately 40 % of body mass in healthy humans [1], transforms chemical energy into mechanical tension, enabling movement. During incremental exercise to exhaustion, the energy demand can rise above 100-fold resting levels, significantly disrupting homeostasis [2,3]. The latter is accompanied by a marked reduction of muscle oxygen pressure (PO_2) and high activation of substrate-level phosphorylation that complements oxidative energy production to match ATP resynthesis with demand. The involvement of substrate-level phosphorylation is intensified when the exercise is performed in hypoxic or ischemic conditions, causing accumulation of lactate, hydron (H^+), and inorganic phosphate (P_i), as well as exacerbating the production of reactive oxygen species (ROS) [2,3], which may lead to oxidative stress and damage. However, skeletal muscle has remarkable plasticity, which relies on tissue remodeling, enabling structural and functional adaptations to cope more efficiently

* Corresponding author. Department of Physical Education, University of Las Palmas de Gran Canaria, Campus Universitario de Tafira s/n, Las Palmas de Gran Canaria, 35017, Spain.
E-mail address: jose.calbet@ulpgc.es (J.A.L. Calbet).
[1] These two authors are co-senior and co-corresponding authors.

https://doi.org/10.1016/j.freeradbiomed.2024.07.012
Received 11 May 2024; Received in revised form 25 June 2024; Accepted 11 July 2024
Available online 14 July 2024

Abbreviations:

AMPKα	AMP-activated protein kinase alpha
ATP	Adenosine triphosphate
AKT	AKT serine/threonine kinase
BECN1	Beclin-1
BSA	Bovine serum albumin
CMA	Chaperone-mediated autophagy
EEF2K	Eukaryotic elongation factor 2 (EEF2) kinase
EEF2	Eukaryotic elongation factor 2
FC1m	60 s after exercise cessation during recovery with free circulation
F_IO_2	Inspired oxygen fraction
FOXO	Forkhead box O
GSK3B	Glycogen synthase kinase 3 beta
H^+	Hydron
HIF1A	Hypoxia inducible factor 1 subunit alpha
HSPA8/HSC70	Heat shock protein family A [Hsp70] member 8
Hyp	Hypoxia
hSKM	Human skeletal muscle
H_2O_2	Hydrogen peroxide
KEAP1	Kelch Like ECH Associated Protein 1
LAMP2A	Lysosomal-associated membrane protein 2A
MAP1LC3B/LC3B	Microtubule associated protein 1 light chain 3 beta
MTOR	Mammalian target of rapamycin
NFE2L2/NRF2	Nuclear factor erythroid-derived 2-like 2
NF-κB	Nuclear Factor-kappa Beta
Nx	Normoxia
Oc1m	60 s after exercise cessation during ischemic recovery
PCr	Phosphocreatine
PHAF1/MYTHO	Phagophore assembly factor 1/macro-autophagy and youth optimizer
PHDs	Prolyl hydroxylases
PPARGC1A/PGC1A	Peroxisome proliferator gamma coactivator 1-alpha
P_i	Inorganic phosphate
P_IO_2	Partial pressure of inspired O_2
PO_2	Oxygen pressure
Post	10 s after exercise cessation during ischemic recovery
Pre	before exercise
ROS	Reactive oxygen species
SQSTM1/p62	Sequestosome 1
SDS	Sodium dodecyl sulphate
ULK1	Unc-51 like autophagy activating kinase 1
UPS	Ubiquitin-proteasome system
$\dot{V}O_2$peak	Peak oxygen consumption
Wmax	Maximal power output at exhaustion

with homeostatic challenges. This process allows the synthesis of new proteins but also requires the renewal of damaged proteins and organelles by autophagy [4–7]. Two main types of autophagy have been characterized in skeletal muscle: macroautophagy and chaperone-mediated autophagy (CMA).

Macroautophagy is particularly active in exercising hSKM. At high intensity, the increase of the AMP:ATP ratio activates adenosine monophosphate-activated protein kinase alpha (AMPKα), which positively upregulates the expression of autophagy genes [8] and phosphorylates and activates unc-51 like autophagy activating kinase 1 (ULK1) at Ser^{556}, initiating macroautophagy [9]. Some studies indicate macroautophagy stimulation following endurance exercise [9–19] and training [12,13,16,20]. Nevertheless, the evidence for markers of autophagosome content and catabolism of cargoreceptors is less conclusive, in particular regarding the protein expression of the microtubule-associated protein 1 light chain 3 beta (MAP1LC3B/LC3B) and sequestosome 1 (SQSTM1/p62) [9,12–16,18,19,21–23]. Little is known regarding phagophore assembly factor 1/macro-autophagy and youth optimizer (PHAF1/MYTHO), a novel regulator of muscle autophagy [24,25], which remains uncharacterized in hSKM.

Chaperone-mediated autophagy is a selective mechanism to degrade soluble damaged proteins and organelles containing the KFERQ-like motif, which are recognized by heat shock protein family A [Hsp70] member 8 (HSPA8/HSC70) [26–28]. The damaged protein and HSPA8 bind to the lysosomal-associated membrane protein 2A (LAMP2A) receptor, eventually resulting in its digestion in the lysosomal lumen. This process is acutely activated in cells under oxidative stress [29] and hypoxia [30]. Reactive oxygen and nitrogen species may elicit CMA since the knockout of nuclear factor erythroid-derived 2-like 2 (NFE2L2/NRF2) reduces LAMP2A mRNA and protein levels in different cell types [31]. Nevertheless, the role and contribution of CMA in exercise-induced skeletal muscle autophagy remains unknown in humans.

The present investigation aimed to determine whether macroautophagy and chaperone-mediated autophagy are activated by acute exercise to exhaustion in hSKM, and ascertain the role played by muscle oxygenation and metabolite accumulation in autophagy signaling. We also aimed at determining the regulation of FOXO, AKT-MTOR and GSK3B under high metabolic stress and its influence on skeletal muscle autophagy signaling. Furthermore, we wanted to describe the temporal course of these signaling responses during the early recovery after exercise and post-exercise ischemia. We hypothesized that exercise would activate macroautophagy and chaperone-mediated autophagy. We also hypothesized that these effects would be more marked when exercise is performed in severe acute hypoxia and further enhanced by post-exercise ischemia. Lastly, we hypothesized that these changes would be reverted to pre-exercise levels early after the cessation of exercise in the muscles recovering with free circulation.

2. Materials and methods

A more detailed description of the methods is provided in the Supplementary Materials and Methods document.

2.1. Subjects

Eleven physically active healthy men were recruited among physical education students (means ± SD; age: 21.5 ± 2.0 years, height: 174 ± 8 cm, body mass: 72.3 ± 9.3 kg, body fat: 16.1 ± 4.9 %, VO_2max in normoxia: 50.7 ± 4.0 mL $kg^{-1}.min^{-1}$). All volunteers were briefed about the aims of the study and the potential risks before providing their written consent. The study was authorized by the Ethical Committee of the University of Las Palmas de Gran Canaria and executed by the Declaration of Helsinki.

For 24 h before the experiments, subjects were asked to avoid ingesting alcohol, caffeine, and taurine-containing drinks and exercise. Likewise, subjects were also requested to maintain a similar dinner the day before the experimental sessions.

2.2. Study design

Even though the current investigation was initially planned to elucidate the mechanisms that limit performance during whole-body exercise in humans [32–35], the study also aimed to determine the

signaling pathways regulated by autophagy and redox stress during exercise and post-exercise ischemia. The NRF2 and NF-κB mechanisms of activation/deactivation during exercise and recovery have been recently described [31,36]. The current article encompasses singular outcomes determining how autophagy signaling is regulated in hSKM during acute exercise in normoxia and severe acute hypoxia, as well as during recovery with either free circulation or ischemia.

2.3. Pre-test and familiarization

Preliminary visits to the laboratory were dedicated to assessing the body composition (dual-energy X-ray absorptiometry [Lunar iDXA] {GE Healthcare, Milwaukee, WI, USA}) [35] and peak oxygen consumption ($\dot{V}O_2$peak) in normoxia (Nx; $F_IO_2 = 0.21$; partial pressure of inspired [P_IO_2] ~143 mmHg) and hypoxia (Hyp; $F_IO_2 = 0.104$; P_IO_2 ~73 mmHg) using a ramp incremental exercise test to exhaustion on a isokinetic ergometer (Lode Excalibur Sport 925900 [Groningen, The Netherlands]) [35]. The respiratory variables were averaged every 20 s to determine the $\dot{V}O_2$peak [37].

2.4. Main experiments and biopsy sampling

A schematic representation of the experimental protocol is presented in Fig. 1. Subjects reported to the laboratory at 8.00 h after fasting from 22:00 h. Upon arrival, they rested supine for 90 min. Then, a baseline muscle biopsy (Pre Nx and Pre Hyp) was taken from one of the m. *vastus lateralis* (assigned randomly) and a cuff (SC10D Hokanson, Bellevue, Washington, USA) connected to a fast cuff inflator (Hokanson, E20 AG101) was placed unilaterally around the thigh biopsied just below the inguinal crease, as previously reported [35]. After a 2-min verification of proper readings and connections, subjects performed an incremental exercise starting with 80 W in normoxia (increasing 30 W every 2 min) and 60 W in hypoxia (increasing 20 W every 2 min) until exhaustion. For the experiment in hypoxia, the air was diluted with medical grade nitrogen, setting the P_IO_2 at ~73 mmHg (equivalent to an altitude of 5300 m above sea level) using an AltiTrainer200 (SMTEC, Nyon, Switzerland in Hyp). In the Nx trial, immediately at exhaustion, the cuff was inflated instantaneously at 300 mmHg to occlude the circulation completely. Exactly 10 s after exhaustion and ischemia, the second biopsy was taken (Post Nx), and 50 s later, while maintaining the cuff inflated, the third biopsy was performed (occluded 1 min, Oc1m Nx, Bergstrom needle introduced with 45° inclination to the head) [38]. The Oc1m biopsy permitted the evaluation of muscle signaling changes after 60-s ischemia when the energy sources depend almost exclusively on substrate-level phosphorylation (ATP, PCr, and glycolysis) while PO_2 decreased immediately to zero [35]. The incremental exercise in hypoxia was performed after similar preparations, obtaining the first baseline biopsy while the subjects breathed room air (normoxia). Then, the volunteers sat on the cycle ergometer and, after 2 min breathing hypoxic gas, the incremental exercise was started. At exhaustion, the cuff was inflated instantaneously while the volunteers were switched to breathe normoxic room air. Ten seconds later, the second biopsy was taken from the cuffed leg (Post Hyp). Immediately, the subjects were carefully moved to a stretcher while maintaining the cuff inflated to obtain the third biopsy exactly after 60 s of ischemia from the cuffed leg (Oc1m Hyp). At the same time, a fourth biopsy was obtained from the contralateral leg (FC1m), which had been recovering with free circulation in normoxia for 60 s. Thus, one leg recovered for 60 s in ischemia and the other with unrestrained free circulation. All muscle samples were immediately frozen in liquid nitrogen and stored at −80 °C.

2.5. Muscle metabolites, protein extraction, and western blotting

The procedures for analyzing the muscle samples are detailed in the Supplementary Materials and Methods document. In short, ~10 mg of muscle were ground and homogenized in urea lysis buffer, supplemented with protease and phosphatase inhibitors. After centrifugation, the total protein content was quantified, and the extract volume was adjusted to a ~5.7 μg/μL final concentration in all muscle protein extracts. Optimal amounts of protein were loaded and tested with antibodies and electrophoresed on SDS-PAGE gels. The proteins were transferred to Immun-Blot polyvinylidene fluoride (PVDF) membranes. Four control samples were processed and run together onto the same gel with the samples from each volunteer. Reactive Brown 10 (R0385, Sigma Aldrich) or Ponceau S (P3504, Sigma Aldrich) were used as total protein staining methods to control for optimal loading and transfer

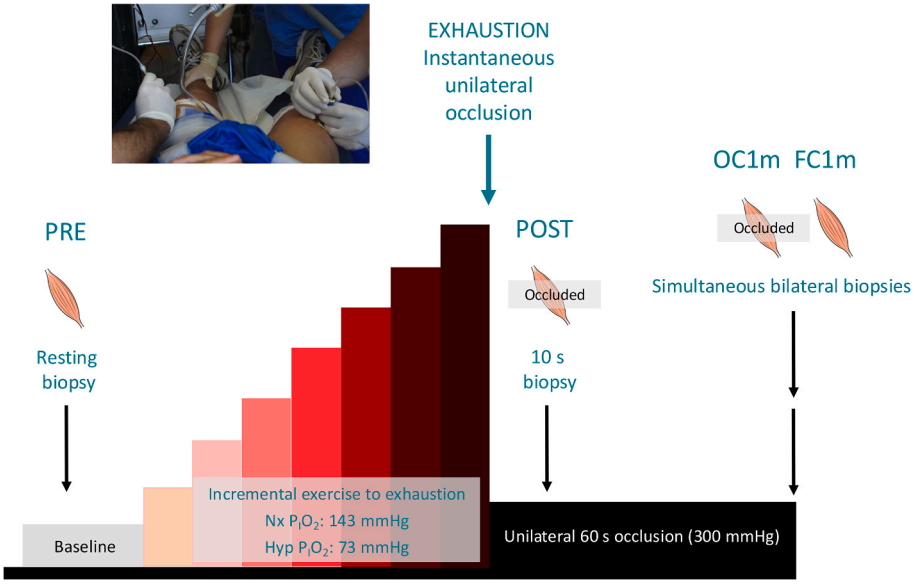

Fig. 1. Schematic representation of the experimental protocol. Eleven volunteers performed an incremental exercise until exhaustion in normoxia ($P_IO_2 = 143$ mmHg) or severe normobaric hypoxia ($P_IO_2 = 73$ mmHg), in random order. A resting skeletal muscle biopsy was obtained from the m. vastus lateralis before warm-up, followed by an incremental exercise test until exhaustion. Upon exhaustion, one leg was occluded with a cuff inflated at 300 mmHg for 60 s. Muscle biopsies were taken from the occluded leg at 10 s and 60 s in both trials (Nx and Hyp). In the test performed in hypoxia, an extra biopsy was obtained at 60 s from the leg recovering with free circulation. During recovery, the subjects breathed normoxic room air.

efficiency. Membranes were blocked and incubated with primary and secondary HRP-conjugated antibodies (see Tables S1 and S2 for details).

2.6. Statistical analysis

Variables were checked for Gaussian distribution using the Shapiro–Wilks test, and when appropriate, data were transformed logarithmically before further analysis. Signaling responses were examined with a two-way 3 x 2 repeated-measures ANOVA with time (Pre, Post, and Oc1m) and F_IO_2 (normoxia and hypoxia) as within-subject factors. The Mauchly's test of sphericity was run before the ANOVAs. In the case of violation of the sphericity assumption, the degrees of freedom were adjusted according to the Huynh and Feldt test. When significant main or interaction effects were observed, pairwise comparisons were adjusted by applying the Holm-Bonferroni procedure. When differences between the post-exercise conditions were not significant, the two pre-exercise conditions were averaged and compared with the four post-exercise points using ischemia (two in normoxia and two in hypoxia). The latter was done by a contrast analysis based on a two-way repeated measures analysis (R Foundation for Statistical Computing, Vienna, Austria, Version: 2023.12.0 Build 369). The occluded and non-occluded legs were compared using a paired two-tailed *t*-test. Linear relationships between variables were determined by applying a linear mixed model, and the Likelihood Ratio Test for the random effects (LRT) was calculated and reported with the marginal and conditional r-squared values. If the residuals of the linear mixed model were not normally distributed, the outcome variable was logarithmically transformed, and the model recalculated. Unless otherwise stated, results are reported as the mean ± standard deviation (SD). Statistical significance was set at $p < 0.05$. Statistical analyses were performed using IBM SPSS Statistics v.29 for Mac (SPSS Inc., Chicago, IL, USA) and jamovi v2.4.8. (The jamovi project 2023, retrieved from https://www.jamovi.org).

3. Results

3.1. Muscle metabolites

The changes in metabolites following exercise have been reported previously [35] and will only be summarized here. In brief, 10 s after the end of the incremental exercise (i.e., at Post), muscle lactate was increased and PCr and ATP decreased. These responses were similar in normoxia (Nx) and hypoxia (Hyp). At the first minute following

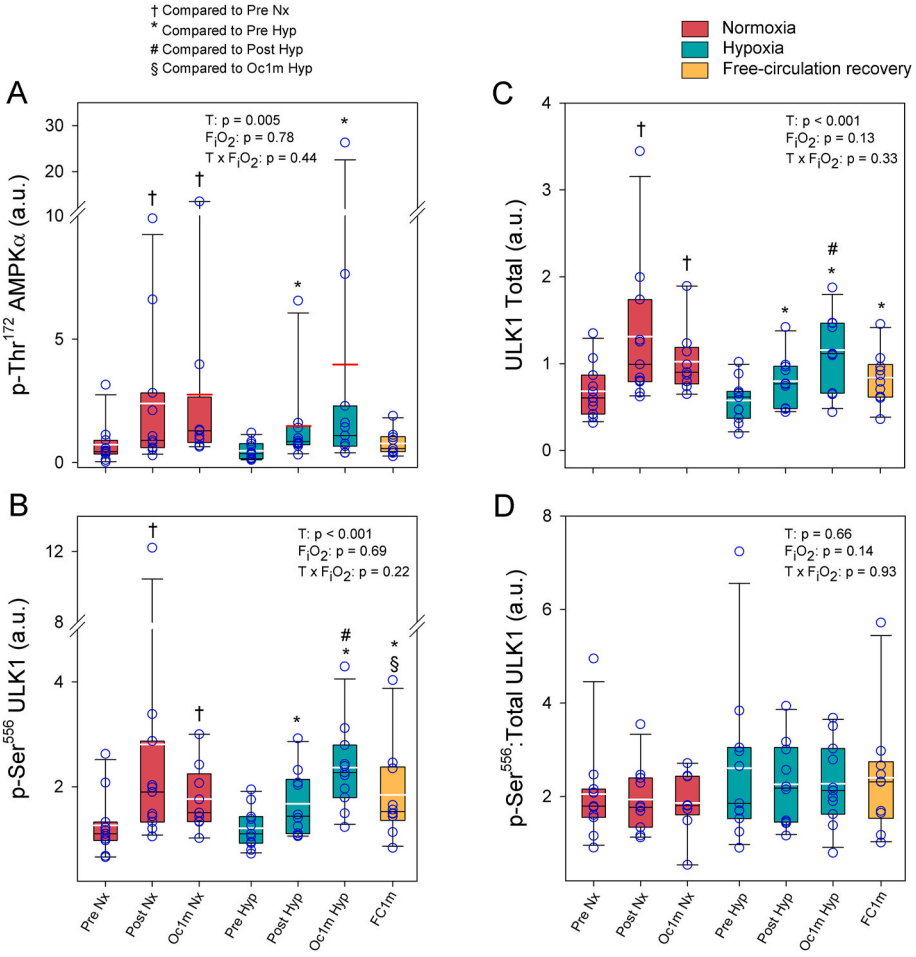

Fig. 2. Protein expression levels of AMPKα and ULK1 signaling in response to incremental exercise to exhaustion in normoxia, severe acute hypoxia, and post-exercise ischemia. Values for (**A**) *p*-Thr^{172} AMPKα, (**B**) *p*-Ser^{556} ULK1, (**C**) ULK1 Total, and (**D**) *p*-Ser^{556}:total ULK1 in arbitrary units (a.u.). The whiskers delimit the 5th and 95th percentiles; the thin and thick horizontal lines correspond to the median and the mean values, respectively; the red horizontal lines correspond to the mean when it lies outside the limits of the box; and the upper and lower ends of the boxes define the 1st and 3rd quartiles, respectively. Nx: Normoxia ($P_IO_2 = 143$ mmHg); Hyp: severe normobaric hypoxia ($P_IO_2 = 73$ mmHg); Pre: before exercise; Post: 10 s after exercise cessation during ischemic recovery; Oc1m: 60 s after exercise cessation during ischemic recovery; FC1m: 60 s after exercise cessation during recovery with free circulation. Individual values are represented with a circle. For panels (A–D), n = 11 for all conditions except for Oc1m Nx (n = 9), Post Hyp and FC1m (n = 10). See Fig. 1 for a detailed description of the experimental phases. The statistical analysis was performed with logarithmically transformed data for all proteins. †$p < 0.05$ vs. Pre Nx; *$p < 0.05$ vs. Pre Hyp; #$p < 0.05$ vs. Post Hyp; §$p < 0.05$ vs. Oc1m Hyp.

exercise, muscle lactate concentration was further increased by 25 % in the leg recovering with ischemia ($p < 0.05$), while it remained unchanged in the leg recovering with free circulation. PCr was reduced by 94 and 48 %, in the occluded (Oc1m) and free-circulation (FC1m) legs, respectively ($p < 0.005$), regardless of inspired oxygen fraction (F_IO_2). Thus, PCr levels were partly restored in the leg recovering with free circulation. Femoral vein PO_2 was 21.1 ± 2.0 and 10.6 ± 2.8 mmHg at maximal power output at exhaustion (Wmax), in Nx and Hyp, respectively ($p < 0.001$).

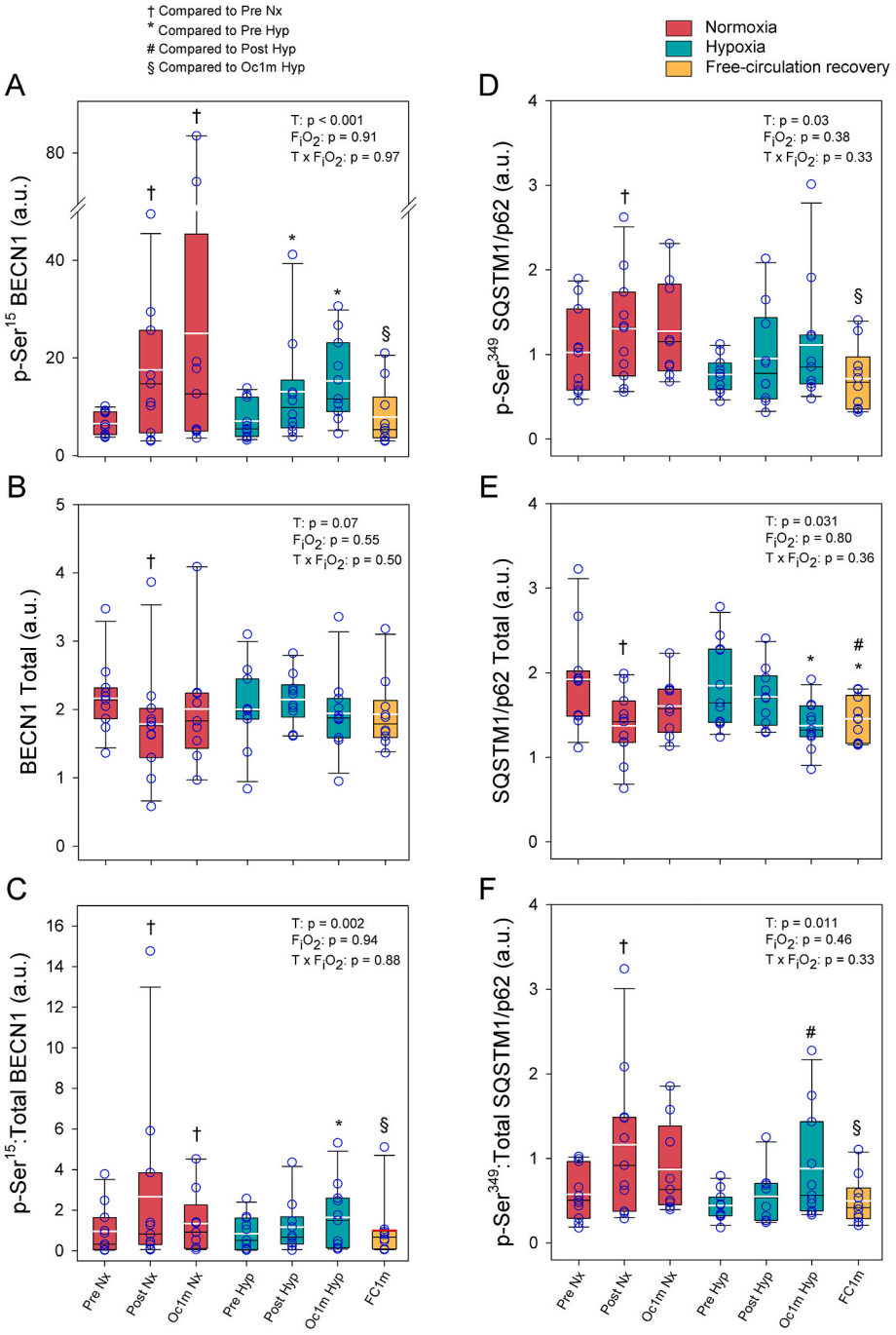

Fig. 3. Protein expression levels of BECN1 and SQSTM1/p62 signaling in response to incremental exercise to exhaustion in normoxia, severe acute hypoxia, and post-exercise ischemia. Values for (**A**) *p*-Ser^{15} BECN1, (**B**) BECN1 Total, (**C**) *p*-Ser^{15}:Total BECN1, (**D**) *p*-Ser^{349} SQSTM1/p62, (**E**) SQSTM1/p62 Total, and (**F**) *p*-Ser^{349}:total SQSTM1/p62 in arbitrary units (a.u.). The whiskers delimit the 5th and 95th percentiles; the thin and thick horizontal lines correspond to the median and the mean values, respectively; the red horizontal lines correspond to the mean when it lies outside the limits of the box; and the upper and lower ends of the boxes define the 1st and 3rd quartiles, respectively. Nx: Normoxia ($P_IO_2 = 143$ mmHg); Hyp: severe normobaric hypoxia ($P_IO_2 = 73$ mmHg); Pre: before exercise; Post: 10 s after exercise cessation during ischemic recovery; Oc1m: 60 s after exercise cessation during ischemic recovery; FC1m: 60 s after exercise cessation during recovery with free circulation. Individual values are represented with a circle. For panels (A–F), n = 11 for all conditions except for Oc1m Nx (n = 9), Post Hyp and FC1m (n = 10). See Fig. 1 for a detailed description of the experimental phases. The statistical analysis was performed with logarithmically transformed data for all proteins, except for *p*-Ser^{349}:total SQSTM1/p62. †$p < 0.05$ vs. Pre Nx; *$p < 0.05$ vs. Pre Hyp; #$p < 0.05$ vs. Post Hyp; §$p < 0.05$ vs. Oc1m Hyp.

3.2. Macroautophagy signaling

Compared to pre-exercise resting values, *p*-Thr^{172} AMPKα (Fig. 2A), *p*-Ser^{556} ULK1 (Fig. 2B), ULK1 total (Fig. 2C), *p*-Ser^{15} BECN1 (Fig. 3A), *p*-Ser^{15} :total BECN1 ratio (Fig. 3C), *p*-Ser^{349} p62 (Fig. 3D), *p*-Ser^{349}:total p62 ratio (Fig. 3F) and MYTHO (Fig. 3E) were significantly increased at Post (1.3 to 4-fold) and Oc1m (1.3 to 8-fold). In contrast, p62 total (Fig. 3E) protein expression was reduced by 19 and 21 % at Post and Oc1m, respectively. Responses in Nx and Hyp were similar.

After 1 min of recovery with free circulation, *p*-Thr^{172} AMPKα, *p*-Ser^{556} ULK1, *p*-Ser^{15} BECN1, *p*-Ser^{15} :total BECN1 ratio, *p*-Ser^{349} p62, *p*-Ser^{349}:total p62 ratio expression returned to pre-exercise levels in the leg

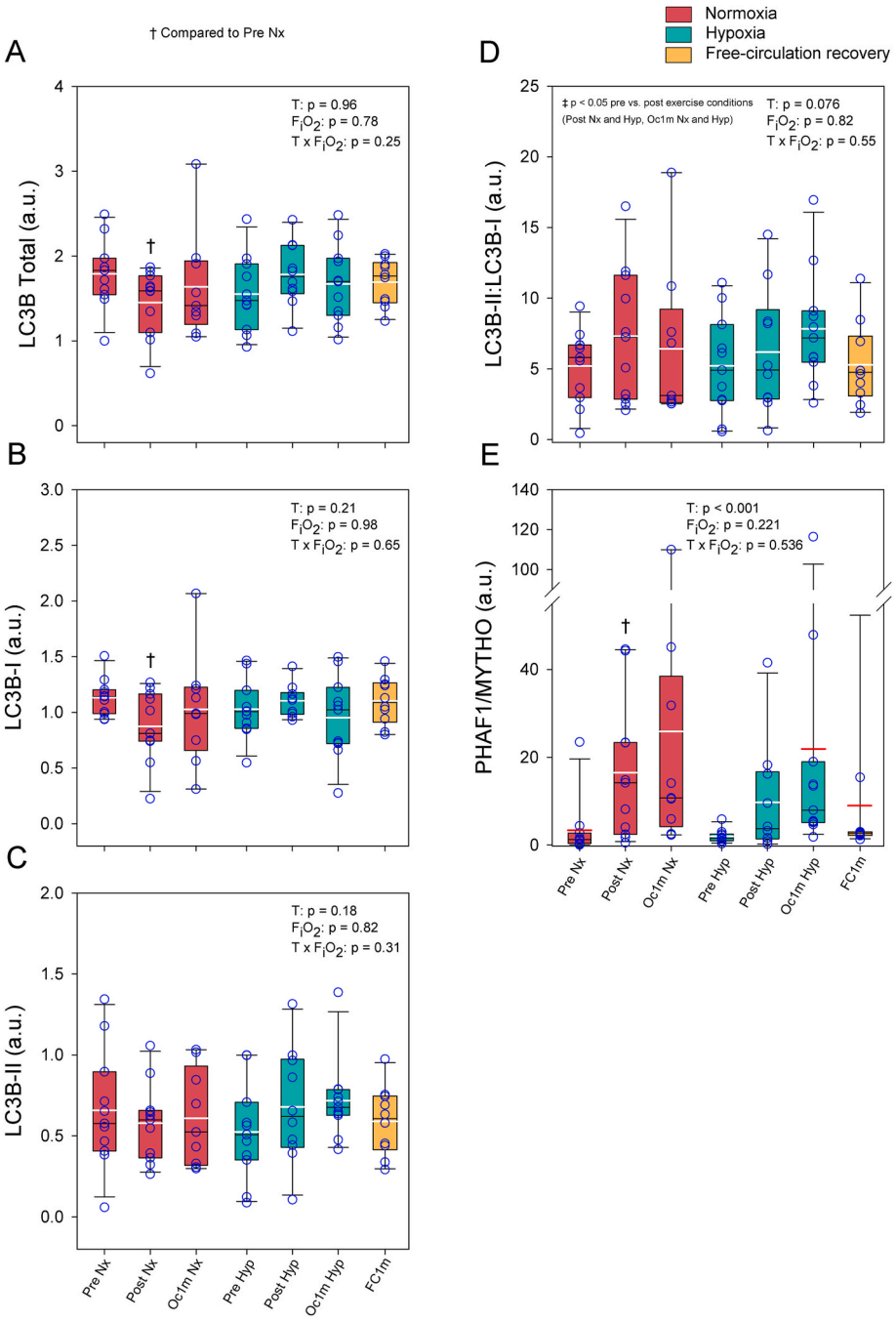

Fig. 4. Protein expression levels of LC3B and MYTHO signaling in response to incremental exercise to exhaustion in normoxia, severe acute hypoxia, and post-exercise ischemia. Values for (**A**) LC3B Total, (**B**) LC3B–I, (**C**) LC3B-II, (**D**) LC3B-II:LC3B–I, and (**E**) MYTHO in arbitrary units (a.u.). The whiskers delimit the 5th and 95th percentiles; the thin and thick horizontal lines correspond to the median and the mean values, respectively; the red horizontal lines correspond to the mean when it lies outside the limits of the box; and the upper and lower ends of the boxes define the 1st and 3rd quartiles, respectively. Nx: Normoxia (P_IO_2 = 143 mmHg); Hyp: severe normobaric hypoxia (P_IO_2 = 73 mmHg); Pre: before exercise; Post: 10 s after exercise cessation during ischemic recovery; Oc1m: 60 s after exercise cessation during ischemic recovery; FC1m: 60 s after exercise cessation during recovery with free circulation. Individual values are represented with a circle. For panels (A–D), n = 11 for all conditions except for Oc1m Nx (n = 9), Post Hyp and FC1m (n = 10). For panels (E), n = 11 for all conditions except for Oc1m Nx (n = 9) and Post Hyp (n = 10). See Fig. 1 for a detailed description of the experimental phases. The statistical analysis was performed with logarithmically transformed data for LC3B Total, LC3B-II and MYTHO. A contrast analysis comparing the two pre with the post exercise (Post Nx and Hyp, Oc1m Nx and Hyp) conditions was performed for LC3B-II:LC3B–I ratio. †p < 0.05 vs. Pre Nx; ‡p < 0.05 two pre vs. the post exercise conditions (Post Nx and Hyp, Oc1m Nx and Hyp).

recovering with free circulation. However, this recovery was incomplete for *p*-Ser^{556} ULK1 and MYTHO, who remained 46 % and 4.5-fold above the resting value after 1 min of recovery with free circulation. One minute after the end of exercise p62 remained similarly reduced in the leg recovering with free circulation and in the leg recovering with ischemia.

Compared to the occluded leg, *p*-Ser^{556} ULK1, ULK1 total, *p*-Ser^{15} BECN1, *p*-Ser^{15} :total BECN1 ratio, *p*-Ser^{349} p62, *p*-Ser^{349}:total p62 ratio and MYTHO were 24–59 % lower in the leg recovering with free circulation. No significant differences were observed between the occluded and non-occluded leg 1 min after exercise in *p*-Thr^{172} AMPKα and p62 total.

The *p*-Ser^{556}:total ULK1 ratio (Fig. 2D), BECN1 total (Fig. 3B), LC3B total (Fig. 4A), LC3B–I (Fig. 4B), LC3B-II (Fig. 4C), and LC3B-II:LC3B–I ratio (Fig. 4D) did not change significantly with ANOVA. However, a contrast analysis comparing the two pre-exercise conditions with those following exercise with ischemia application (Post Nx and Hyp, Oc1m Nx and Hyp) was performed to increase the statistical power and determine whether there was an exercise effect. This analysis revealed that LC3B-II:LC3B–I ratio was significantly increased by exercise 1.4-fold.

3.3. Chaperone-mediated autophagy

Compared to pre-exercise, LAMP2A (Fig. 5A) was increased 1.2 and 1.3-fold at Post and Oc1m, respectively, while HSPA8 (Fig. 5B) was reduced by 25 % at Oc1m, with similar responses in Nx and Hyp. After 1 min of recovery with free circulation, LAMP2A and HSPA8 expression returned to pre-exercise levels. Compared to the occluded leg, HSPA8 was 1.4-fold higher in the leg recovering with free circulation.

3.4. FOXOs signaling

Compared to pre-exercise, *p*-Ser^{256} FOXO1 (Fig. 6A) and *p*-Ser^{256}:total FOXO1 ratio (Fig. 6C) were increased at Post (2.2 and 2.4-fold, respectively) and Oc1m (2.6 and 3.2-fold, respectively). Compared to pre-exercise, *p*-Ser^{253} FOXO3 (Fig. 6D) and FOXO3 total (Fig. 6E) were increased by 1.8 and 1.3-fold, respectively, at Oc1m, while FOXO1 total (Fig. 6B) protein expression was significantly reduced by 13 % at Oc1m. Responses in Nx and Hyp were similar.

After 1 min of recovery with free circulation, *p*-Ser^{256} FOXO1, FOXO1 total, *p*-Ser^{256}:total FOXO1 ratio, *p*-Ser^{253} FOXO3, FOXO3 total expression returned to pre-exercise levels in the leg recovering with free circulation, being 30–65 % lower in the leg recovering with free-circulation compared with the occluded leg.

The ratio *p*-Ser^{253}:total FOXO3 (Fig. 6F) did not change significantly with ANOVA. However, a contrast analysis comparing the two pre with the post-exercise (Post Nx and Hyp, Oc1m Nx and Hyp) conditions indicated that the ratio *p*-Ser^{253}:total FOXO3 increased significantly by 27 % after exercise.

3.5. Protein synthesis and protein elongation signaling

Compared to pre-exercise, *p*-Ser^{9} GSK3B (Fig. 7A) and *p*-Ser^{473} AKT (Fig. 7B) were reduced at Post (20 and 54 %, respectively) and Oc1m (23 and 65 %, respectively). Phospho-Thr^{56} EEF2 (Fig. 7C) and *p*-Thr^{56}:total EEF2 ratio (Fig. 7E) were increased at Post (3.5 and 3.6-fold, respectively) and Oc1m (3.4 and 4.2-fold, respectively). Responses in Nx and Hyp were similar.

After 1 min of recovery with free circulation, *p*-Ser^{473} AKT remained 73 % below the resting value in the leg recovering with free circulation. In contrast, *p*-Thr^{56} EEF2 and *p*-Thr^{56}:total EEF2 ratio remained 4.3 and 6-fold above the resting value, while *p*-Ser^{9} GSK3B returned to Pre-exercise levels. No significant differences were observed between the occluded and non-occluded leg in *p*-Ser^{473} AKT, *p*-Thr^{56} EEF2, *p*-Thr^{56}:total EEF2 ratio and *p*-Ser^{9} GSK3B. Phospho-Ser^{2448} MTOR (Fig. 7F) and EEF2 total (Fig. 7D) did not change significantly.

3.6. Hypoxia signaling

Compared to pre-exercise, hydroxy-Pro^{564} HIF1A (Fig. 8A) and hydroxy-Pro^{564}:total HIF1A ratio (Fig. 8C) were increased at Post (1.9 and 1.7-fold, respectively) and Oc1m (1.8 and 1.7-fold, respectively), with a similar response in Nx and Hyp.

After 1 min of recovery with free circulation, hydroxy-Pro^{564} HIF1A expression returned to resting values, while hydroxy-Pro^{564}:total HIF1A

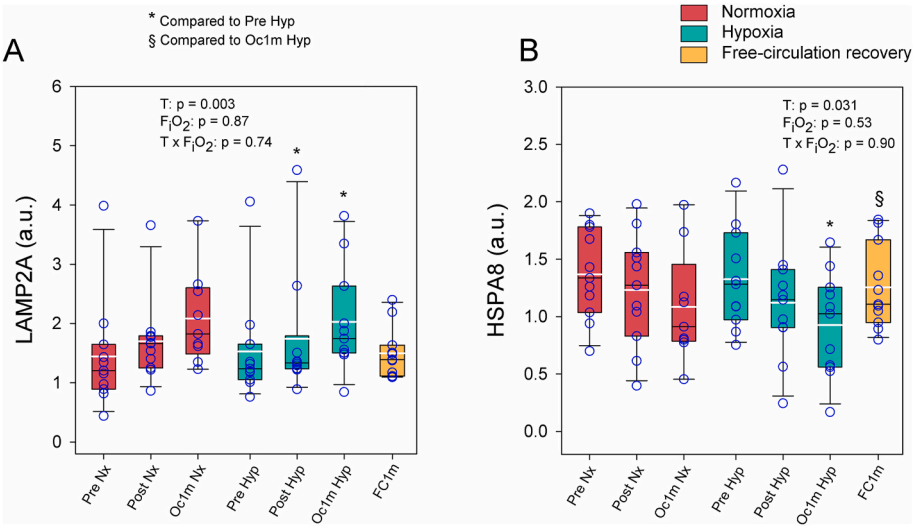

Fig. 5. Protein expression levels of LAMP2A and HSPA8 signaling in response to incremental exercise to exhaustion in normoxia, severe acute hypoxia, and post-exercise ischemia. Values for (**A**) LAMP2A and (**B**) HSPA8 in arbitrary units (a.u.). The whiskers delimit the 5th and 95th percentiles; the thin and thick horizontal lines correspond to the median and the mean values, respectively; and the upper and lower ends of the boxes define the 1st and 3rd quartiles, respectively. Nx: Normoxia (P_IO_2 = 143 mmHg); Hyp: severe normobaric hypoxia (P_IO_2 = 73 mmHg); Pre: before exercise; Post: 10 s after exercise cessation during ischemic recovery; Oc1m: 60 s after exercise cessation during ischemic recovery; FC1m: 60 s after exercise cessation during recovery with free circulation. Individual values are represented with a circle. For panel (A), n = 11 for all conditions except for Oc1m Nx (n = 9) and Post Hyp (n = 10). For panel (B), n = 11 for all conditions except for Oc1m Nx (n = 9). See Fig. 1 for a detailed description of the experimental phases. *p < 0.05 vs. Pre Hyp; §p < 0.05 vs. Oc1m Hyp.

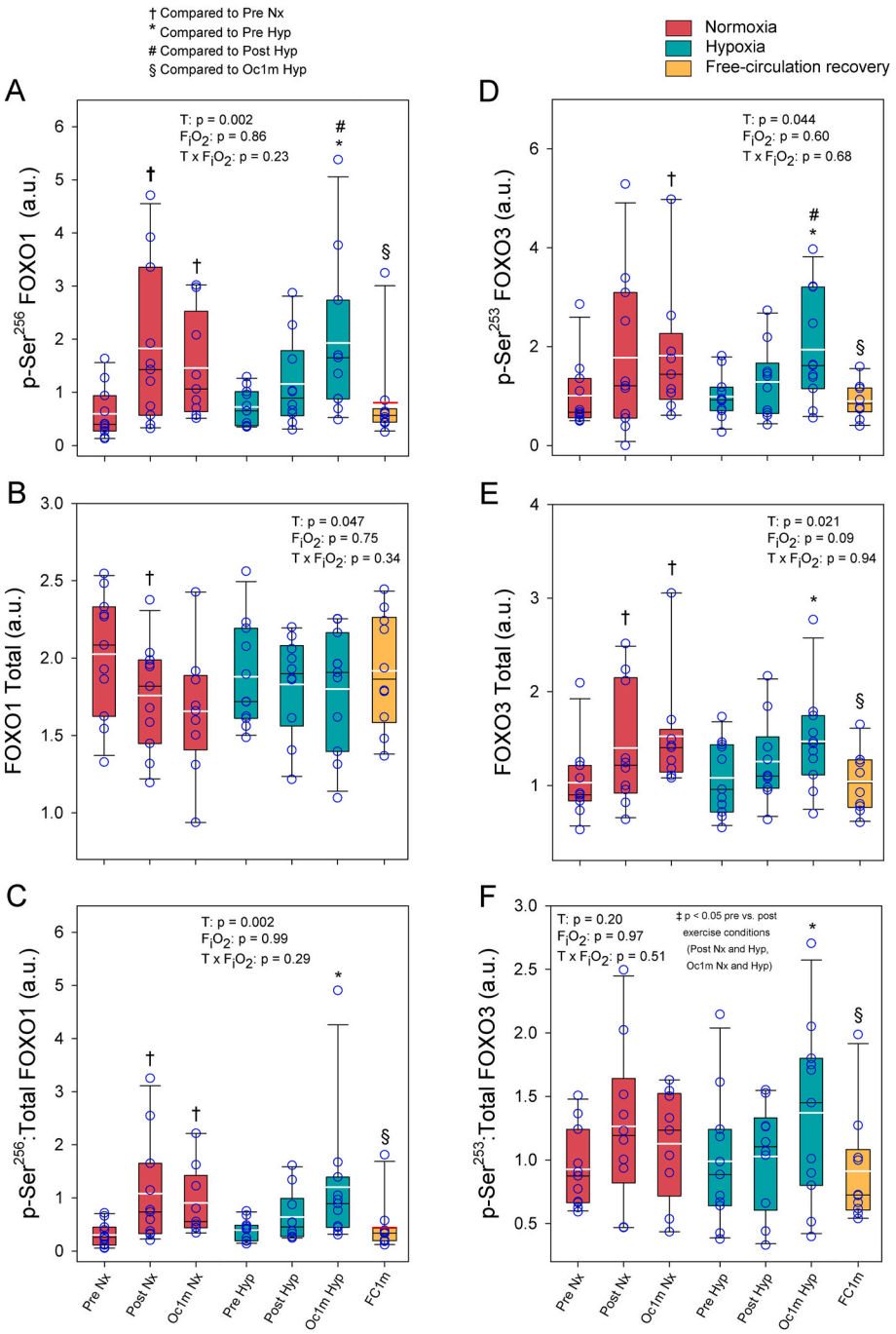

Fig. 6. Protein expression levels of FOXOs signaling in response to incremental exercise to exhaustion in normoxia, severe acute hypoxia, and post-exercise ischemia. Values for (**A**) *p*-Ser^{256} FOXO1, (**B**) FOXO1 total, (**C**) *p*-Ser^{256}:total FOXO1, (**D**) *p*-Ser^{253} FOXO3, (**E**) FOXO3 total, and (**F**) *p*-Ser^{253}:total FOXO3 in arbitrary units (a.u.). The whiskers delimit the 5th and 95th percentiles; the thin and thick horizontal lines correspond to the median and the mean values, respectively; the red horizontal lines correspond to the mean when it lies outside the limits of the box; and the upper and lower ends of the boxes define the 1st and 3rd quartiles, respectively. Nx: Normoxia (P_IO_2 = 143 mmHg); Hyp: severe normobaric hypoxia (P_IO_2 = 73 mmHg); Pre: before exercise; Post: 10 s after exercise cessation during ischemic recovery; Oc1m: 60 s after exercise cessation during ischemic recovery; FC1m: 60 s after exercise cessation during recovery with free circulation. Individual values are represented with a circle. For panels (A–D), n = 11 for all conditions except for Oc1m Nx (n = 9), Post Hyp and FC1m (n = 10). For panels (E) and (F), n = 11 except for Oc1m Nx (n = 9), Post Nx, Post Hyp and FC1m (n = 10). See Fig. 1 for a detailed description of the experimental phases. The statistical analysis was performed with logarithmically transformed data for *p*-Ser^{256} FOXO1, *p*-Ser^{256}: total FOXO1 and FOXO3 total. A contrast analysis comparing the two pre with the post exercise (Post Nx and Hyp, Oc1m Nx and Hyp) conditions was performed for *p*-Ser^{253}:total FOXO3. †p < 0.05 vs. Pre Nx; *p < 0.05 vs. Pre Hyp; #p < 0.05 vs. Post Hyp; §p < 0.05 vs. Oc1m Hyp; ‡p < 0.05 two pre vs. the post-exercise conditions (Post Nx and Hyp, Oc1m Nx and Hyp).

ratio was reduced by 28 % compared to Pre-exercise. Compared to the occluded leg, hydroxy-Pro^{564}:total HIF1A ratio and hydroxy-Pro^{564} HIF1A were 66 and 77 % lower in the leg recovering with free circulation, respectively.

No significant changes were observed in HIF1A total (Fig. 8B) protein content with the ANOVA. A contrast analysis comparing the two pre- and the post-exercise (Post Nx and Hyp, Oc1m Nx and Hyp) conditions showed that exercise increased significantly HIF1A total by 1.2-fold.

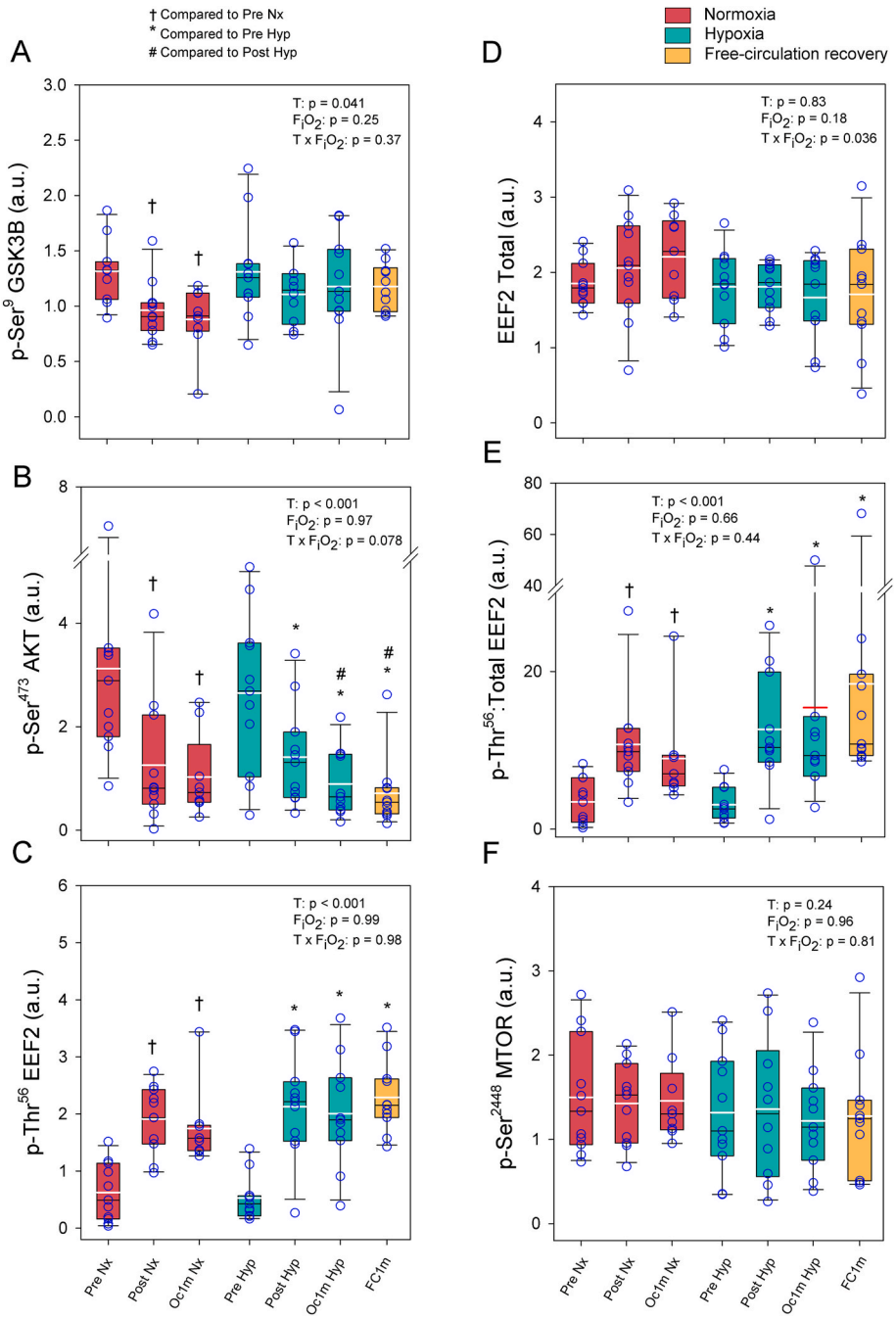

Fig. 7. Protein expression levels of the GSK3B, AKT, EEF2, and MTOR signaling in response to incremental exercise to exhaustion in normoxia, severe acute hypoxia, and post-exercise ischemia. Values for (**A**) *p*-Ser^{9} GSK3B, (**B**) *p*-Ser^{473} AKT, (**C**) *p*-Thr^{56} EEF2, (**D**) EEF2 Total, (**E**) *p*-Thr^{56}:Total EEF2 and (**F**) *p*-Ser^{2448} MTOR in arbitrary units (a.u.). The whiskers delimit the 5th and 95th percentiles; the thin and thick horizontal lines correspond to the median and the mean values, respectively; the red horizontal lines correspond to the mean when it lies outside the limits of the box; and the upper and lower ends of the boxes define the 1st and 3rd quartiles, respectively. Nx: Normoxia (P_IO_2 = 143 mmHg); Hyp: severe normobaric hypoxia (P_IO_2 = 73 mmHg); Pre: before exercise; Post: 10 s after exercise cessation during ischemic recovery; Oc1m: 60 s after exercise cessation during ischemic recovery; FC1m: 60 s after exercise cessation during recovery with free circulation. Individual values are represented with a circle. For panel (A), n = 11 for all conditions except for Oc1m Nx (n = 9), Post Hyp and FC1m (n = 10). For panels (B–E), n = 11 for all conditions except for Oc1m Nx (n = 9). For panel (F), n = 11 for all conditions except for Oc1m Nx (n = 9) and Post Hyp (n = 10). See Fig. 1 for a detailed description of the experimental phases. The statistical analysis was performed with logarithmically transformed data for *p*-Ser^{473} AKT, *p*-Thr^{56} EEF2, and *p*-Thr^{56}:Total EEF2. †p < 0.05 vs. Pre Nx; *p < 0.05 vs. Pre Hyp; #p < 0.05 vs. Post Hyp.

3.7. PGC1A expression

Compared to Pre, *p*-Ser^{571} PGC1A (Fig. 8D) was increased by 1.9 and 2.5-fold at Post and Oc1m, respectively, with similar responses in Nx and Hyp. After 1 min of recovery with free circulation *p*-Ser^{571} PGC1A returned to Pre-exercise values and was 51 % lower than in the occluded leg.

3.8. Linear associations

Positive linear associations were observed between *p*-Thr^{172} AMPKα and ULK1 phosphorylation at Ser^{556} (R^2 marginal = 0.48, R^2 conditional = 0.98, intercept and slope random effect LRT p < 0.001) (Fig. S1A) and PGC1A phosphorylation at Ser^{571} (R^2 marginal = 0.67, R^2

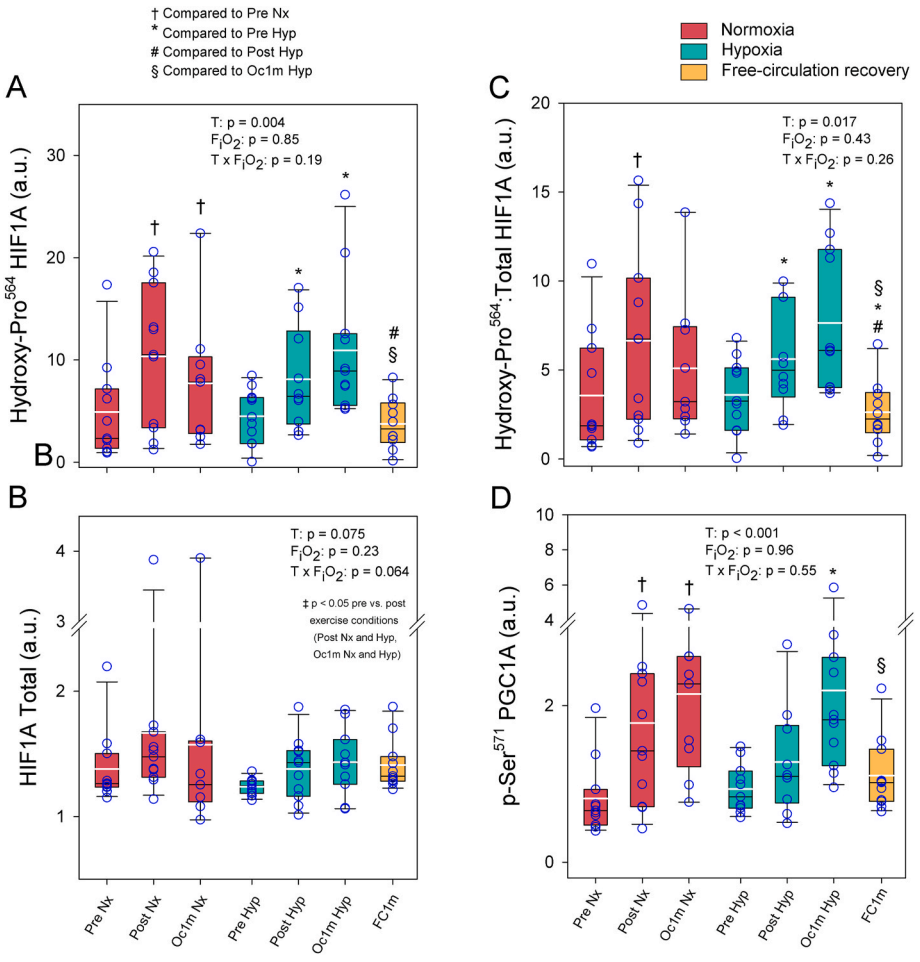

Fig. 8. Protein expression levels of the HIF1A and PGC1A signaling in response to incremental exercise to exhaustion in normoxia, severe acute hypoxia, and post-exercise ischemia. Values for (**A**) Hydroxy-Pro^{564} HIF1A, (**B**) HIF1A Total, (**C**) Hydroxy-Pro^{564}:Total HIF1A, (**D**) *p*-Ser^{571} PGC1A in arbitrary units (a.u.). The whiskers delimit the 5th and 95th percentiles; the thin and thick horizontal lines correspond to the median and the mean values, respectively; and the upper and lower ends of the boxes define the 1st and 3rd quartiles, respectively. Nx: Normoxia (P_IO_2 = 143 mmHg); Hyp: severe normobaric hypoxia (P_IO_2 = 73 mmHg); Pre: before exercise; Post: 10 s after exercise cessation during ischemic recovery; Oc1m: 60 s after exercise cessation during ischemic recovery; FC1m: 60 s after exercise cessation during recovery with free circulation. Individual values are represented with a circle. For panels (A) and (C), n = 11 for all conditions except for Oc1m Nx (n = 9), Post Hyp and FC1m (n = 10). For panel (B), n = 11 for all conditions except for Oc1m Nx (n = 9). For panel (D), n = 11 for all conditions except for Oc1m Nx (n = 9) and Post Hyp (n = 10). See Fig. 1 for a detailed description of the experimental phases. The statistical analysis was performed with logarithmically transformed data for HIF1A Total and *p*-Ser^{571} PGC1A. A contrast analysis comparing the two pre with the post exercise (Post Nx and Hyp, Oc1m Nx and Hyp) conditions was performed for HIF1A total. †p < 0.05 vs. Pre Nx; *p < 0.05 vs. Pre Hyp; #p < 0.05 vs. Post Hyp; §p < 0.05 vs. Oc1m Hyp; ‡p < 0.05 two pre vs. the post exercise conditions (Post Nx and Hyp, Oc1m Nx and Hyp).

conditional = 0.91, intercept and slope random effect LRT p = 0.046) (Fig. S1B). ULK1 phosphorylation at Ser^{556} was linearly associated to *p*-Ser^{15} BECN1 (R^2 marginal = 0.43, R^2 conditional = 0.84, intercept and slope random effect LRT p = 0.003) (Fig. S1C). MYTHO was linearly associated with the LC3B-II:LC3B–I ratio (R^2 marginal = 0.09, R^2 conditional = 0.46, intercept effect LRT p < 0.001) (Fig. S1D). Likewise, a linear association was observed between *p*-Ser^{40} NRF2 and LAMP2A (R^2 marginal = 0.05, R^2 conditional = 0.67, intercept effect LRT p < 0.001) (Fig. S1E).

Representative immunoblots of all proteins studied are presented in Fig. 9.

4. Discussion

This study showed that macroautophagy and chaperone-mediated autophagy (CMA) signaling pathways are activated by acute exercise to exhaustion in human skeletal muscle (hSKM) with a similar response in normoxia and severe acute hypoxia, even though femoral vein PO_2 at exhaustion was halved at exhaustion in hypoxia (Nx: 21.1 ± 2.0 Vs. Hyp: 10.6 ± 2.8 mmHg). It is worth noting that the level of hypoxia elicited is close to the limit of tolerance for non-altitude acclimatized humans. Macroautophagy remained activated during the 1 min post-exercise occlusion while it was restored to almost pre-exercise conditions in the leg recovering with free circulation just 1 min after the end of exercise, demonstrating that reversion of the exercise-mediated activation of macroautophagy requires O_2. The present findings indicated that macroautophagy signaling might be activated through upregulation of the AMPKα-ULK1, lowered phosphorylation levels of AKT and GSK3B, and unchanged *p*-Ser^{2448} MTOR. The latter was accompanied by increased signaling promoting autophagosome formation and cargo degradation, as indicated by the rise of the LC3B-II:LC3B–I ratio and MYTHO, and the decrease of SQSTM1/p62 total protein content. Chaperone-mediated autophagy was facilitated, as indicated by the observed increase in LAMP2A (a critical step for CMA) with exercise and ischemia. Moreover, the observed upregulation of the inhibitory phosphorylations of FOXO1 and FOXO3 indicates that there was no activation of FOXO signaling with exhaustive exercise, ischemia or systemic hypoxia, indicating that FOXOs are not necessary for macroautophagy

nor CMA activation in hSKM. Concomitantly with the activation of protein degradation signaling through macroautophagy and CMA, protein synthesis was blunted, as shown by the inhibition of protein elongation (see Fig. 10 for a graphical summary).

The signaling responses in this study were similar in normoxia and hypoxia; however, within 1 min after exercise cessation, most of the signaling changes were reverted to pre-exercise levels in the leg recovering with free circulation. This observation has important methodological implications for future studies since to capture the exercise-induced signaling response, muscle biopsies should be performed immediately at exhaustion or delayed a few seconds, but in the latter case, ischemia should be applied to maintain the exercise-induced signaling.

4.1. AMPKα-ULK1-triggered macroautophagy signaling initiation during high-intensity exercise and ischemia is unchanged under severe acute hypoxia in human skeletal muscle

The present investigation showed that an acute bout of exercise until exhaustion followed by 60s of total immediate ischemia increased

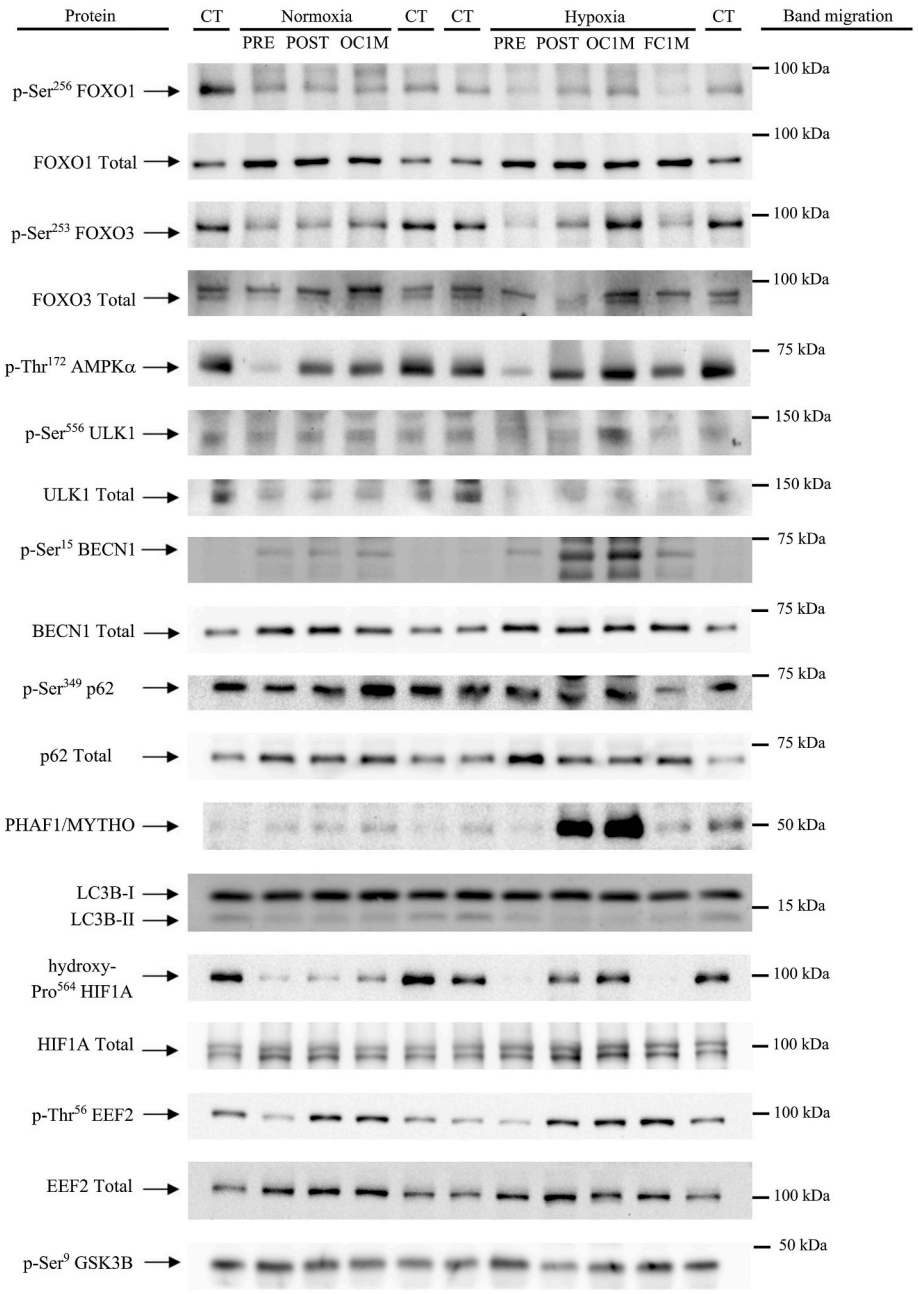

Fig. 9. Immunoblots and total amount of protein loaded (Reactive Brown Staining) from a representative subject of the study. Images from top to bottom: *p*-Ser^{256} FOXO1, FOXO1 total, *p*-Ser ^{253} FOXO3, FOXO3 total, *p*-Thr^{172} AMPKα, *p*-Ser^{556} ULK1, ULK1 total, *p*-Ser^{15} BECN1, BECN1 total, *p*-Ser^{349} SQSTM1/p62, SQSTM1/p62 total, PHAF1/MYTHO, LC3B–I, LC3B-II, hydroxy-Pro^{564} HIF1A, HIF1A total, *p*-Thr^{56} EEF2, EEF2 total, *p*-Ser^{9} GSK3B, LAMP2A, HSPA8, *p*-Ser^{473} AKT, *p*-Ser^{2448} MTOR, *p*-Ser^{571} PGC1A, and Reactive Brown (as total protein loading control). A detailed description of experimental phases is included in Fig. 1. CT, non-intervention healthy human sample included in quadruplicate onto each gel as a loading control. Normoxia: test performed with P_IO_2 = 143 mmHg; Hypoxia: test performed with P_IO_2 = 73 mmHg; Pre: before exercise; Post: 10 s after the end of exercise with ischemic recovery; Oc1m: 60 s after the end of exercise with ischemic recovery; FC1m: 60 s after exercise cessation during recovery with free circulation. The molecular weight standard markers closest to the migration of the band are indicated on the right side of the panel.

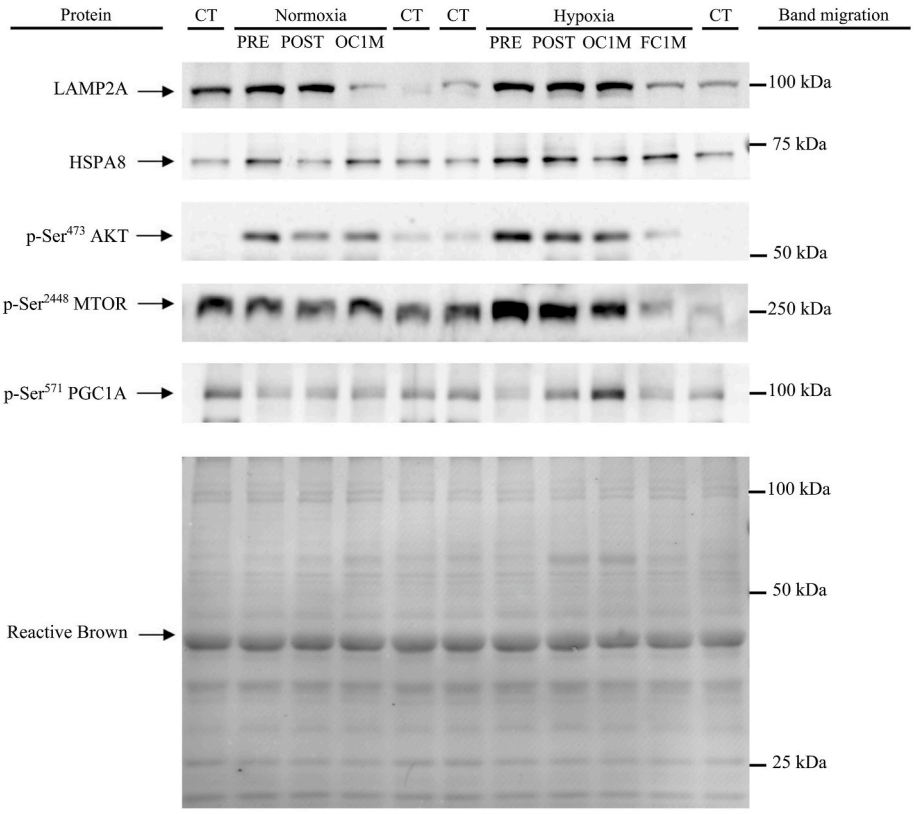

Fig. 9. (*continued*).

macroautophagy initiation signaling. Our results concur with the reported upregulation of *p*-Thr^{172} AMPKα and the subsequent phosphorylation of ULK1 at residues Ser^{317} or Ser^{556} seen after cycling for 60 min at 50–70 % peak oxygen consumption ($\dot{V}O_2$peak) [11, 13, 15, 17] and ultra-endurance exercise [14]. The observed positive linear association between *p*-Thr^{172} AMPKα and *p*-Ser^{556} ULK1 further supports the activation of ULK1 by AMPKα. No additional macroautophagy signaling activation was observed in hypoxia compared to normoxia, despite the very low femoral vein PO_2 values attained during exercise in hypoxia in the present investigation. This agrees with previous studies in moderate hypoxia (12 % O_2) [17]. As a novelty, we have shown that the application of leg ischemia at exhaustion maintained upregulated these signals similarly in Nx and Hyp. This is consistent with the activation of NRF2-KEAP1 [31] and nuclear factor-kappa Beta (NF-κB)-depending signaling in this experiment [36], which were neither upregulated with ischemia nor hypoxia. Thus, the levels of ROS and metabolite accumulation reached at the end of incremental exercise in normoxia are sufficient to stimulate macroautophagy signaling in human skeletal muscle maximally.

4.2. BECN1, LC3B, and SQSTM1/p62 signaling in response to acute exercise to exhaustion and ischemia

The complex BECN1/PIK3C3 is considered a marker of membrane nucleation, mediating the phagophore formation [39]. The activation of BECN1 Ser^{15} phosphorylation by ULK1 is crucial for disassembling the BECN1-BCL2 complex [40] and phagophore formation [7,18]. In agreement, a linear positive association was observed in the present investigation between *p*-Ser^{556} ULK1 and BECN1 Ser^{15} phosphorylation. As a novelty, we have seen a notable increase in BECN1 Ser^{15} phosphorylation after exercise and ischemia. In the present study, no changes were observed in the levels of total BECN1 after incremental exercise to exhaustion and recovery. This outcome concurs with the unchanged BECN1 protein expression reported after 60 min cycling at 50–60 % $\dot{V}O_2$peak [9,13] and ultra-endurance exercise [14,21,22].

LC3B has been widely considered an indirect marker of macroautophagy activity and autophagosome formation in rodent and human experimental models; however, changes in LC3B should be interpreted with caution [41]. In rodents, higher LC3B-II and LC3B-II:LC3B–I ratio values indicate increased macroautophagy and autophagosome content [16]. In human studies involving exercising for 30–120 min at 50–70 % of $\dot{V}O_2$peak, an elevated macroautophagy signaling is typically associated with a reduced LC3B-II:LC3B–I ratio, primarily driven by increased LC3B-II degradation [9,11,12,15,16]. In contrast, in the present investigation, the LC3B-II:LC3B–I ratio was increased after exercise due to reduced free LC3B–I but unchanged LC3B-II levels, which is compatible with increased lipidation activity to LC3B-II and autophagosome formation. SQSTM1/p62 harbors an LC3-interacting region domain involved in the specific transport of SQSTM1/p62-tagged substrates within the autophagosome [42]. Most studies on human skeletal muscle have reported no changes in SQSTM1/p62 total protein levels following prolonged exercise at 50–70 % of $\dot{V}O_2$peak [9,13,15,16] or ultra-endurance exercise [14]. In agreement with a potential increase of autophagic flux, SQSTM1/p62 was reduced after exercise, likely due to p62 autophagosome co-degradation [43]. The observed increased p62 Ser^{349} phosphory-lation further supports an increased macroautophagy flux, which facilitates p62 co-degradation with KEAP1 [31,42,44]. Our results combined with previous studies, indicate that a significant reduction of p62 after exercise is only seen at intensities above 80 % of $\dot{V}O_2$peak.

4.3. PHFA1/MYTHO, the novel macroautophagy biomarker, is upregulated in response to acute exercise and ischemia in human skeletal muscle

Our results have shown that MYTHO, a novel FOXO-dependent gene barely detectable at rest, experienced a marked upregulation after

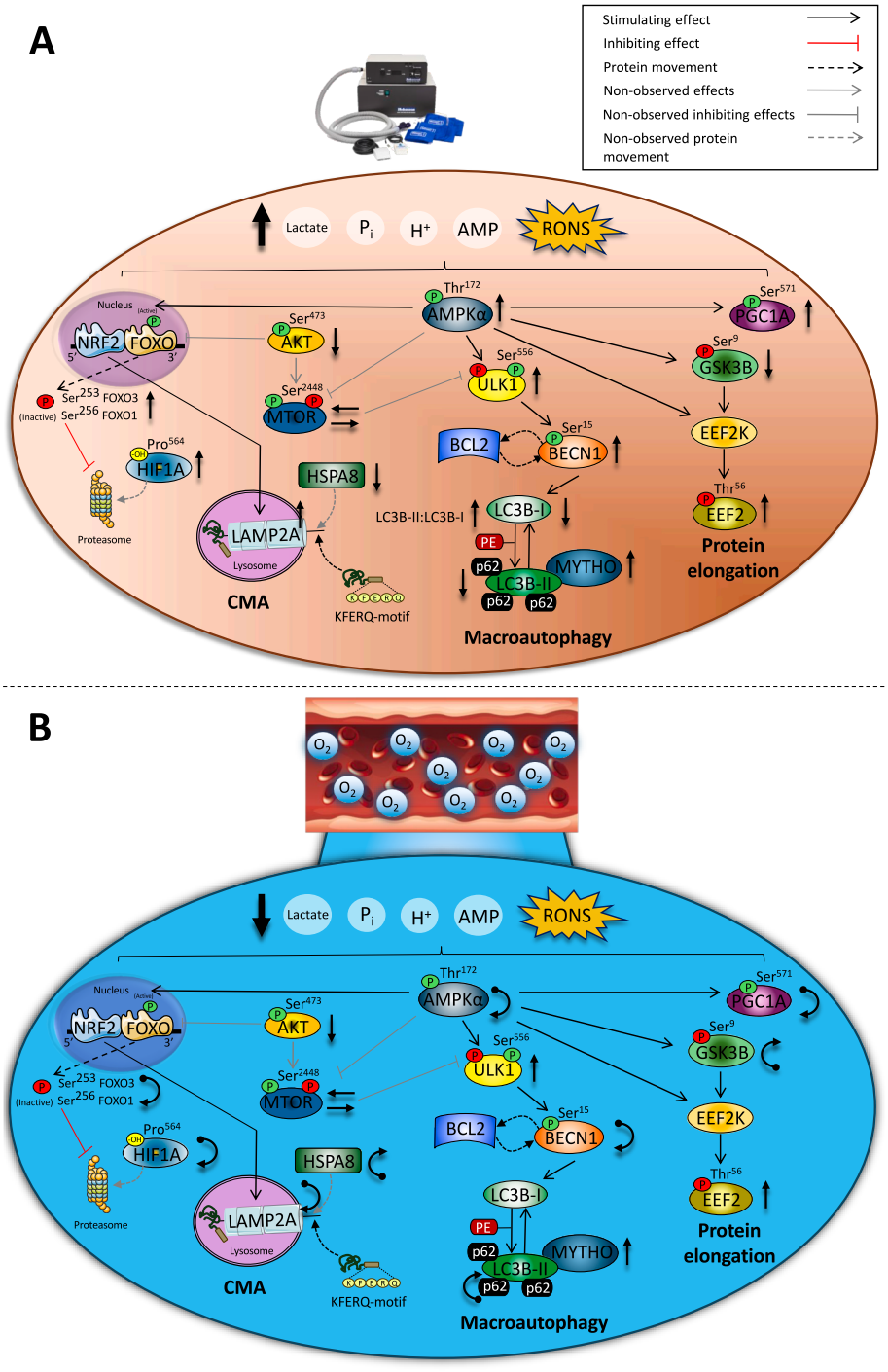

(caption on next page)

Fig. 10. Schematic representation of the signaling pathways regulating autophagy activation in skeletal muscle in response to exercise to exhaustion in normoxia and severe normobaric hypoxia followed by ischemia-reperfusion. (A) Low levels of AMP:ATP ratio and ROS evoked by incremental exercise to exhaustion activate AMPKα. Phosphorylated AMPKα induces autophagy initiation by directly phosphorylating ULK1 at Ser^{556}. ULK1 stimulates phagophore formation through BECN1 Ser^{15} phosphorylation, which is crucial for disassembling the BECN1-BCL2 complex. Expansion of the autophagosome requires LC3B–I lipidation to LC3B-II. Ubiquitinated tagged substrates are recognized by SQSTM1/p62, which targets the material to the growing autophagosome by binding to LC3B-II. MYTHO/PHAF1 harbors an LC3 interacting region, which may regulate the elongation step of autophagosome formation. Chaperone-mediated autophagy degrades proteins containing the KFERQ motif, which are recognized by HSPA8. The damaged protein and HSPA8 are identified by the LAMP2A receptor, being digested in the lysosomal lumen. Protein synthesis is inhibited after exercise and ischemia as seen by a declined AKT phosphorylation at Ser^{473} and unchanged MTOR. MTOR, when active, phosphorylates and inhibits ULK1. EEF2K, a kinase that regulates protein elongation, is activated by active GSK3B, leading to increased phosphorylation of EEF2 at Thr^{56} and inhibition of protein elongation. Inhibitory phosphorylation of FOXO leads to its nuclear exclusion and inactivation. Insufficient energy availability could compromise proteasomal degradation, leading to the accumulation of hydroxylated HIF1A. AMPKα also positively regulates the activity of PGC1A, which increases the transcriptional activity of autophagy-related genes. **(B)** Most of the upregulated biomarkers rapidly reverted to pre-exercise levels within 60 s of free-circulation recovery, indicating a fast regulation of autophagy following the cessation of exercise, which depends on muscle reoxygenation. All proteins assessed are similarly regulated after exercise in normoxia and severe acute hypoxia. Stimulating/inhibiting effects are represented by black/red connecting lines. Protein movements are depicted with black dashed lines. Actions known but not observed/assessed in this investigation are depicted in grey (with dashed lines indicating a protein movement). The black arrows shown beside each biomarker illustrate the magnitude of the protein expression changes (increased/decreased/maintained/returned to pre-exercise levels) in this investigation.

exercise in normoxic and hypoxic conditions. In the present study, exercise resulted in FOXO inhibition, suggesting that the exercise induction of MYTHO does not require FOXO activation. In agreement, it has been reported that FOXO1 is not required for MYTHO induction with fasting in rodents [25]. In the present study, other molecular mechanisms should explain the increased MYTHO expression after high-intensity exercise. In our investigation, the observed increase in the LC3B-II:LC3B–I ratio and upregulation of MYTHO after acute exercise and ischemia may be linked. Studies in knockout MYTHO mice's skeletal muscles showed reduced autophagosome formation accompanied by lowered RNA levels of BECN1 and reduced LC3B-II:LC3B–I ratio [24,25]. Rodent experiments have shown that the interaction between MYTHO and LC3B is crucial for the elongation step of autophagosome formation, emphasizing the pivotal role of MYTHO in the autophagy machinery within skeletal muscle [45]. This is further supported by the positive association between the LC3B-II:LC3B–I ratio and MYTHO observed in the present investigation. As a novelty, our study demonstrates that muscle oxygenation is required to downregulate the exercise-induced elevation of MYTHO, which occurs quickly upon cessation of muscle contractions. This downregulation is necessary to prevent hyperactivation of autophagy [24,25]. We did not observe changes in MTOR protein levels, and there was a decline in AKT phosphorylation at Ser^{473}, indicating inhibition of protein synthesis.

4.4. LAMP2A and HSPA8 in response to high-intensity exercise, ischemia, and hypoxia induces chaperone-mediated autophagy signaling

The limiting step of CMA is the availability of the LAMP2A receptor at the lysosomal membrane, which is regulated by NRF2 [28,46], linking oxidative damage with CMA induction [47]. In mouse hepatocytes, knockout of NRF2 reduces LAMP2A mRNA and protein levels [47]. The present study provides for the first time evidence for upregulation of both NRF2 [31] and LAMP2A protein expression in response to high-intensity exercise and post-exercise ischemia in human skeletal muscle, underscored by the linear positive association observed here between *p*-Ser^{40} NRF2 and LAMP2A. HSPA8 selectively recognizes substrates with KFERQ-like motifs for lysosomal degradation [48,49] and is active under oxidative stress conditions [29]. We have previously shown that this exercise model elicits oxidative stress and increased protein carbonylation [50]. Thus, the results are compatible with increased degradation of muscle proteins with KFERQ-like motifs, facilitated by oxidative stress and the reduced cellular PO_2 observed at near maximal exercise in normoxia and hypoxia. The marked increase in LAMP2A observed here with exercise should have facilitated this process. The induction of macroautophagy in our exercise model should have elicited the fusion of autophagosomes and lysosomes, contributing to increased intracellular lysosomal pH, a known mechanism stimulating HSPA8 degradation [26]. Besides, the present study demonstrates that reduced HSPA8 and increased LAMP2A protein levels with exercise are rapidly reverted during recovery with free circulation.

4.5. Greater levels of muscle hypoxia do not enhance exercise-induced autophagy signaling or HIF1A levels

Production of ROS in skeletal muscle is exacerbated by exercise in hypoxia, likely due to a higher activation of the anaerobic metabolism and metabolic acidosis [50]. In contrast to our hypothesis, autophagy signaling markers were similar at exhaustion in normoxia and severe acute hypoxia, indicating that the activation was already maximal in normoxia or that the additional reduction in cellular PO_2 during exercise in hypoxia was not enough to stimulate autophagy further. These findings are consistent with the outcomes presented by Moberg et al. during submaximal exercise at a lower level of hypoxia than used in the present investigation [17].

Proline hydroxylation is enzymatically catalyzed by prolyl hydroxylases (PHDs), where oxygen acts as a co-substrate [51]. Under normoxic PO_2 levels, the PHDs catalyze the hydroxylation of HIF1A at residue Pro^{564}, targeting it for the E3 ubiquitin ligase and the subsequent proteasome-mediated degradation [52]. Here, we have observed a substantial increase in HIF1A hydroxylation at exhaustion, which remained elevated during ischemia. This change is compatible with the reported reduction of Von Hippel-Lindau tumor suppressor protein with exercise [33,53]. Other conceivable mechanisms accounting for the accumulation of hydroxylated HIF1A following incremental exercise could include a decrease in its proteasomal degradation rate due to insufficient energy availability [54]. This concurs with the observed inactivation of FOXO. Moreover, in the present investigation, the increase in the hydroxy-Pro^{564}: total HIF1A ratio was not attenuated in hypoxia despite the very low partial pressure of oxygen in arterial blood (P_aO_2) values (~33 mmHg near exhaustion) [33]. This could be because skeletal muscle is designed to work under the very low PO_2 levels reached during high-intensity exercise and forceful isometric contractions (which cause ischemia) [52].

4.6. Protein synthesis and elongation downregulation accompany the activation of autophagy

At low energy levels, AMPKα inhibits MTOR [55], suppressing protein synthesis. The latter impedes MTOR phosphorylation of ULK1 at Ser^{757}, which would inhibit ULK1 [56]. MTOR phosphorylation levels remained unchanged following exercise and ischemia in the present investigation, which concurs with the observed lack of activation of its upstream kinase AKT. Notably, our study participants had undergone a fasting period exceeding 12 h. These findings are consistent with Schwalm et al. [15], highlighting AKT activation's dependency on the fed state. They reported robust AKT stimulation in the fed state but

observed no such stimulation in AKT after exercise in a fasted state. Additionally, previous investigations in mouse skeletal muscle have documented a decline in AKT activity during fasting conditions [57,58]. The unchanged *p*-Ser^{2448} MTOR levels after post-exercise and ischemia in the present investigation concurs with Brandt et al. [13], which report unchanged *p*-Ser^{2448} MTOR after moderate cycling for 60 min at 60 % $\dot{V}O_2$peak. Furthermore, high-volume exercises, such as ultra-endurance activities, led to unchanged [14] and decreased [14,22] protein expression levels of MTOR and AKT.

Protein elongation is controlled by EEF2 [59], which EEF2K inhibits through Thr^{56} phosphorylation of EEF2 [54]. EEF2K, a calcium/calmodulin-dependent kinase (or CaMKIII), is activated by AMPKα [60,61] and GSK3B [62] and inhibited through proline hydroxylation [54]. In the present investigation, the inhibitory phosphorylation of EEF2 was markedly increased after exercise to a similar extent in normoxia and hypoxia. This concurs with the reported similar activation of AMPKα in both conditions [17] and the similar inhibition of GSK3B reported here. Therefore, it indicates downregulation of protein synthesis and elongation, which is expected due to the reduced energy charge during high-intensity exercise until exhaustion [35].

4.7. Upregulation of PGC1A by AMPKα and CaMKII following exercise and ischemia: another potential mechanism to stimulate exercise-induced autophagy

The peroxisome proliferator gamma coactivator 1-alpha (PPARGC1A/PGC1A) is the master regulator of mitochondrial biogenesis [63–66], preserving mitochondrial quality and promoting the transcription of macroautophagy genes [64,67–71]. Calmodulin-dependent protein kinase II and AMPKα are upstream regulators of PGC1A, which the current investigation has found upregulated after exercise and ischemia, both in normoxia and hypoxia [31,36]. Notably, these changes are reverted to their pre-exercise levels within just 1 min of muscle oxygenation [31,36]. The higher levels of intracellular Ca^{2+} and the heightened energy demand, along with the accumulation of metabolites during acute exercise, may lead to the phosphorylation of PGC1A by AMPKα [72], increasing its transcriptional activity [72], which may manifest a few hours after exercise [73].

4.8. Rapid reversal of exercise-induced autophagy activation by immediate post-exercise tissue reoxygenation

Another original feature of this study was the application of post-exercise total ischemia (cuff pressure: 300 mmHg) just immediately after the end of the incremental exercise to exhaustion in both tests. This approach allowed us to capture fast signaling events that may be reversed by cessation of muscle contractions combined with post-exercise hyperemia. During the first 3–5 s of the occlusion, the O_2 stores (O_2 trapped in capillary blood and bound to myoglobin) undergo depletion due to the heightened stimulation of oxidative phosphorylation [35,74]. This was evidenced by the fast reduction and stable plateau of muscle oxygenation measured by near-infrared spectroscopy, as previously reported [35]. Importantly, the initial post-exercise muscle biopsy was performed 10 s following exercise cessation, when the muscle conditions closely resembled those experienced at exhaustion while the cuff was inflated. The same leg was re-biopsied after 60 s of occlusion, while simultaneously an additional biopsy was obtained from the contralateral extremity, which recovered with a free circulation. This approach enabled a direct comparison between the occluded and non-occluded leg. During the 60 s occlusion, the energy metabolism continued to be active in the occluded leg, primarily relying on the energy derived from glycolysis. The latter resulted in lactate, H^+, P_i, and free creatine accumulation, while the concentration of ATP remained at the same level reached at exhaustion, i.e., ~-80 % of the concentration observed before exercise [35]. Despite the increased cytosolic acidification during the 60 s occlusion, no significant changes in signaling were observed between the 10th and the 60th s of post-exercise ischemia in the occluded leg. This suggests that autophagy signaling reached its maximum level at exhaustion and remained at that level during the ischemic period. The production of ROS during the 60 s of ischemia is also improbable, given the absence of oxygen supply from the 10th to the 60th second in the occluded leg [75]. In agreement, Gallego et al., using data from the same experiment, revealed that the redox-sensitive NRF2-KEAP1 pathway is not further activated from the 10th to the 60th s of post-exercise ischemia [31]. Moreover, most of the protein signaling changes elicited by exercise returned to the pre-exercise status just 60 s after the end of exercise in the leg recovering with free circulation, even though muscle lactate and H^+ remained almost at the same level reached at exhaustion [35]. In contrast, P_i and Cr were reduced due to PCr resynthesis during the 60 s recovery with free circulation but without reaching pre-exercise values [35]. This suggests that muscle lactate or acidification is not crucial in initiating or sustaining signaling activation. Instead, the large increase of P_i, accompanied by almost depletion of PCr during ischemia, may have inhibited the phosphatases [76], preserving during ischemia the phosphorylation levels of the proteins assessed here. The rapid restoration of autophagy signaling to pre-exercise levels requires oxygen and is essential to avoid the hazards associated with excessive and uncontrolled proteolytic stimulation [18,77,78].

4.9. Oxygenation and signaling in resting human skeletal muscle

The effect of oxygenation in resting skeletal muscle signaling has barely been researched in humans. A few studies have explored the impact of prolonged ischemia on muscle signaling, particularly in patients undergoing surgical procedures such as total knee arthroplasty (TKA) [79,80]. Leurcharusmee et al. [79] applied three cycles of 5-min ischemia followed by 5-min reperfusion just before performing a TKA in patients. They obtained the muscle biopsies from the *vastus medialis* 30 min after the last ischemia and upon release of the surgical tourniquet, which was inflated at 100 mmHg above systolic arterial pressure. In Leurcharusmee et al. [79], mitochondrial fusion proteins (MFN2 and OPA1) were increased at the onset of reperfusion. At the same time, no significant changes were observed in 4-HNE, SOD2, TNF, IL6, *p*-Ser^{616} DRP1:DRP1, MFN1, PGC1A, ETC complex I–V, CYCS, and cleaved CASP3/CASP3 expression between the end of ischemia and reperfusion [79]. Nevertheless, the baseline signaling was not measured, impeding the comparison between normal resting conditions and ischemia. Bailey et al. [80] obtained *vastus lateralis* muscle biopsies before, after ~43 min of ischemia (tourniquet pressurized above 300 mmHg), and after ~16 min of reperfusion in 70-year-old osteoarthritis patients (8 females and 4 males) during TKA. Ischemia was associated with the upregulation of the MAFbx and MURF1 [80]. Shadgan et al. [81] reported increased protein oxidation in *peroneus tertius* muscle biopsies obtained before and immediately after ~43 min of surgical ischemia (300 mmHg pressure). There is no data on the human skeletal muscle signaling responses to ischemia in healthy humans since previous research has been carried out in patients with osteoarthritis-related muscle atrophy [82] or in the context of other kinds of orthopedic surgery [81]. Direct comparisons between these studies and the present findings are challenging due to different baseline physiological conditions and a lack of information regarding biopsy timing in previous studies. Moreover, no other studies have analyzed the skeletal muscle signaling responses to post-exercise ischemia.

4.10. The role of ROS in autophagy signaling in skeletal muscle

During exercise, ROS are primarily produced by nicotinamide adenine dinucleotide phosphate oxidase 2 (NOX2) and mitochondria [83,84], yet their direct involvement in skeletal muscle autophagy remains unclear. In our study, the application of immediate and complete

post-exercise ischemia trapped ROS and metabolites while muscle oxygen was depleted within 3–5 s, preventing early recovery, as previously reported [35]. In the present investigation, muscle lactate and H^+ were increased with exercise and ischemia [35]. Hydrogen ions can interact with superoxide radicals to form hydrogen peroxide (H_2O_2), which, under acidic conditions, can react with Fe^{2+} via the Fenton reaction, producing hydroxyl radicals (OH^-) [85]. In C2C12 cells, high doses of H_2O_2 activate AMPKα, increasing autophagy and PGC1A transcriptional activation [86,87]. After incremental exercise and ischemia, the highly acidic intra-cellular environment may have facilitated ROS production, AMPK Thr^{172} phosphorylation, autophagy, and PGC1A phosphorylation at Ser^{571} in our experimental conditions. Nutrient deprivation in Chinese Hamster Ovary (CHO) cells triggers mitochondrial H_2O_2 production, inhibiting Atg4 and prolonging autophagosome elongation by preventing LC3B-II delipidation [88]. We observed higher levels of LC3B-II:LC3B–I due to decreased LC3B–I, which may indicate increased LC3B-II lipidation activity. Talbert et al. [89] showed that increased mitochondrial ROS levels in a rat model of disuse muscle atrophy inhibit AKT/MTOR signaling, activating key proteolytic systems [89]. In our study, AKT activation decreased, and MTOR remained unchanged after incremental exercise, likely due to increased post-exercise and ischemia ROS production, prompting autophagy activation. Moreover, ROS are known to facilitate the translocation of FOXO to the nucleus [90]. However, the ROS levels in our study may not have been sufficient to activate FOXOs, as their activation typically occurs under pathological conditions associated with muscle atrophy [91]. ROS also upregulate NRF2 [31], a key promoter of p62 expression [92]. Despite upregulated transcription, low p62 levels indicated degradation by lysosomal proteases [93]. NRF2 also upregulates LAMP2A receptor [94], the primary regulator of CMA [28,46]. Thus, by stimulating autophagy and elimination of damaged organelles, ROS downregulate their own production.

In conclusion, our findings indicate that macroautophagy and CMA were similarly upregulated during exercise to exhaustion in normoxia and severe acute hypoxia. Furthermore, ROS produced during incremental exercise and ischemia may activate macroautophagy and CMA but not FOXOs. We have also shown increased expression of the novel autophagy PHAF1/MYTHO biomarker in human skeletal muscle in response to exercise in normoxia, hypoxia, and post-exercise ischemia. Our study does not support a critical involvement of FOXOs in exercise-induced autophagy. We have also provided evidence for a concurrent activation of autophagy with inhibition of protein synthesis. Additionally, we have demonstrated that exercise-induced autophagy activation was not enhanced by severe acute hypoxia and was reversed within 60 s of recovery as long as the circulation was intact.

4.11. Strengths and limitations

The main strength of the present investigation relies on the uniqueness of its experimental design, which allows it to address early signaling events elicited by exercise in humans. Besides, we have assessed these responses during exercise in normoxia and severe acute hypoxia close to the tolerable limit for humans. Our biopsies were obtained just 10 s after the end of incremental exercise and immediately after occlusion, with accurate timing. Other studies report the biopsy at rest and time 0 h (after exercise), but no accurate time details are provided. Although the principal limitation of this study is the absence of a direct assessment of autophagic flux, which cannot be performed in humans, we provide the combination of several indirect markers of autophagy, which are compatible with an increased autophagic flux with high-intensity exercise. Another limitation of the present study is that due to the small amount of tissue available, biomarkers of oxidative stress were not assessed. However, we have provided extensive evidence for ROS-induced signaling [31,36]. Our findings are based on Western blot analyses, which show high variability. Nevertheless, the latter was accounted for by the statistical analysis and proper normalization. It should be highlighted that recent research has shown that the autophagy response to exercise in humans is different from that observed in rodents, further emphasizing the relevance of this contribution. A final strength of this study is the comprehensive assessment of skeletal muscle signaling through the combination of experimental conditions and the thorough assessment of physiological and biochemical variables.

Disclosure statement

No potential conflict of interest was reported by the authors.

Data availability statement

The data that support the findings of this study are available on request from the co-senior author, MMR. The data are not publicly available due to ethical restrictions.

CRediT authorship contribution statement

Miriam Martinez-Canton: Writing – original draft, Validation, Resources, Methodology, Investigation, Formal analysis, Data curation, Conceptualization. **Victor Galvan-Alvarez:** Writing – review & editing, Validation, Methodology, Investigation, Formal analysis, Data curation. **Angel Gallego-Selles:** Writing – review & editing, Validation, Resources, Methodology, Investigation, Formal analysis, Data curation, Conceptualization. **Miriam Gelabert-Rebato:** Writing – review & editing, Investigation, Formal analysis. **Eduardo Garcia-Gonzalez:** Writing – review & editing, Methodology, Investigation, Formal analysis, Conceptualization. **Juan Jose Gonzalez-Henriquez:** Writing – review & editing, Validation, Methodology, Formal analysis, Data curation. **Marcos Martin-Rincon:** Writing – review & editing, Visualization, Validation, Supervision, Resources, Project administration, Methodology, Investigation, Formal analysis, Data curation, Conceptualization. **Jose A.L. Calbet:** Writing – review & editing, Visualization, Validation, Supervision, Resources, Project administration, Methodology, Investigation, Funding acquisition, Formal analysis, Conceptualization.

Declaration of competing interest

The authors declare that they have no known competing financial interests or personal relationships that could have appeared to influence the work reported in this paper.

Acknowledgements

This study was financed by grants from the Ministerio de Economía y Competitividad (DEP2017-86409-C2-1-P; PID2021-125354OB-C21). AGS is a beneficiary of the Catalina Ruiz training grant program for researchers from the Consejería de Economía, Conocimiento y Empleo, and the Fondo Social Europeo. The funders had no role in study design, data collection and analysis, decision to publish, or preparation of the manuscript. The technical assistance by Jose Navarro de Tuero is greatly appreciated.

Appendix A. Supplementary data

Supplementary data to this article can be found online at https://doi.org/10.1016/j.freeradbiomed.2024.07.012.

References

[1] R.L. Leibel, M. Rosenbaum, J. Hirsch, Changes in energy expenditure resulting from altered body weight, N. Engl. J. Med. 332 (10) (1995) 621–628.
[2] D. Morales-Alamo, B. Guerra, J.G. Ponce-Gonzalez, A. Guadalupe-Grau, A. Santana, M. Martin-Rincon, et al., Skeletal muscle signaling, metabolism, and performance during sprint exercise in severe acute hypoxia after the ingestion of antioxidants, J. Appl. Physiol. 123 (5) (2017) 1235–1245.

[3] M. Gelabert-Rebato, J.C. Wiebe, M. Martin-Rincon, V. Galvan-Alvarez, D. Curtelin, M. Perez-Valera, et al., Enhancement of exercise performance by 48 hours, and 15-day supplementation with mangiferin and luteolin in men, Nutrients 11 (2) (2019).
[4] Y. Nishimura, I. Musa, L. Holm, Y.C. Lai, Recent advances in measuring and understanding the regulation of exercise-mediated protein degradation in skeletal muscle, Am. J. Physiol. Cell Physiol. 321 (2) (2021) C276–C287.
[5] J. Sin, A.M. Andres, D.J. Taylor, T. Weston, Y. Hiraumi, A. Stotland, et al., Mitophagy is required for mitochondrial biogenesis and myogenic differentiation of C2C12 myoblasts, Autophagy 12 (2) (2016) 369–380.
[6] C. He, R. Sumpter Jr., B. Levine, Exercise induces autophagy in peripheral tissues and in the brain, Autophagy 8 (10) (2012) 1548–1551.
[7] C. He, M.C. Bassik, V. Moresi, K. Sun, Y. Wei, Z. Zou, et al., Exercise-induced BCL2-regulated autophagy is required for muscle glucose homeostasis, Nature 481 (7382) (2012) 511–515.
[8] M. Martin-Rincon, D. Morales-Alamo, J.A.L. Calbet, Exercise-mediated modulation of autophagy in skeletal muscle, Scand. J. Med. Sci. Sports 28 (3) (2018) 772–781.
[9] A.B. Møller, M.H. Vendelbo, B. Christensen, B.F. Clasen, A.M. Bak, J.O. Jørgensen, et al., Physical exercise increases autophagic signaling through ULK1 in human skeletal muscle, J. Appl. Physiol. 118 (8) (2015) 971–979.
[10] Y. Arribat, N.T. Broskey, C. Greggio, M. Boutant, S. Conde Alonso, S.S. Kulkarni, et al., Distinct patterns of skeletal muscle mitochondria fusion, fission and mitophagy upon duration of exercise training, Acta Physiol. 225 (2) (2019) e13179.
[11] R. Kruse, A.J. Pedersen, J.M. Kristensen, S.J. Petersson, J.F. Wojtaszewski, K. Højlund, Intact initiation of autophagy and mitochondrial fission by acute exercise in skeletal muscle of patients with Type 2 diabetes, Clin. Sci. (Lond.) 131 (1) (2017) 37–47.
[12] A.M. Fritzen, A.B. Madsen, M. Kleinert, J.T. Treebak, A.M. Lundsgaard, T. E. Jensen, et al., Regulation of autophagy in human skeletal muscle: effects of exercise, exercise training and insulin stimulation, J. Physiol. 594 (3) (2016) 745–761.
[13] N. Brandt, T.P. Gunnarsson, J. Bangsbo, H. Pilegaard, Exercise and exercise training-induced increase in autophagy markers in human skeletal muscle, Phys. Rep. 6 (7) (2018) e13651.
[14] M. Moberg, G. Hendo, M. Jakobsson, C.M. Mattsson, E. Ekblom-Bak, M. Flockhart, et al., Increased autophagy signaling but not proteasome activity in human skeletal muscle after prolonged low-intensity exercise with negative energy balance, Phys. Rep. 5 (23) (2017).
[15] C. Schwalm, C. Jamart, N. Benoit, D. Naslain, C. Prémont, J. Prévet, et al., Activation of autophagy in human skeletal muscle is dependent on exercise intensity and AMPK activation, Faseb. J. 29 (8) (2015) 3515–3526.
[16] J. Botella, N.A. Jamnick, C. Granata, A.J. Genders, E. Perri, T. Jabar, et al., Exercise and training regulation of autophagy markers in human and rat skeletal muscle, Int. J. Mol. Sci. 23 (5) (2022).
[17] M. Moberg, W. Apro, O. Horwath, G. van Hall, S.J. Blackwood, A. Katz, Acute normobaric hypoxia blunts contraction-mediated mTORC1- and JNK-signaling in human skeletal muscle, Acta Physiol. 234 (2) (2022) e13771.
[18] M. Martin-Rincon, A. Pérez-López, D. Morales-Alamo, I. Perez-Suarez, P. de Pablos-Velasco, M. Perez-Valera, et al., Exercise mitigates the loss of muscle mass by attenuating the activation of autophagy during severe energy deficit, Nutrients 11 (11) (2019).
[19] W.J. Smiles, M.S. Conceicao, G.D. Telles, M.P. Chacon-Mikahil, C.R. Cavaglieri, F. C. Vechin, et al., Acute low-intensity cycling with blood-flow restriction has no effect on metabolic signaling in human skeletal muscle compared to traditional exercise, Eur. J. Appl. Physiol. 117 (2) (2017) 345–358.
[20] D.A. Cardinale, K.D. Gejl, K.G. Petersen, J. Nielsen, N. Ørtenblad, F.J. Larsen, Short-term intensified training temporarily impairs mitochondrial respiratory capacity in elite endurance athletes, J. Appl. Physiol. 131 (1) (2021) 388–400.
[21] C. Jamart, N. Benoit, J.M. Raymackers, H.J. Kim, C.K. Kim, M. Francaux, Autophagy-related and autophagy-regulatory genes are induced in human muscle after ultraendurance exercise, Eur. J. Appl. Physiol. 112 (8) (2012) 3173–3177.
[22] C. Jamart, M. Francaux, G.Y. Millet, L. Deldicque, D. Frere, L. Feasson, Modulation of autophagy and ubiquitin-proteasome pathways during ultra-endurance running, J. Appl. Physiol. 112 (9) (2012) 1529–1537.
[23] E. Masschelein, R. Van Thienen, G. D'Hulst, P. Hespel, M. Thomis, L. Deldicque, Acute environmental hypoxia induces LC3 lipidation in a genotype-dependent manner, Faseb. J. 28 (2) (2014) 1022–1034.
[24] J.-P. Leduc-Gaudet, A. Franco-Romero, M. Cefis, A. Moamer, F.E. Broering, G. Milan, et al., MYTHO is a novel regulator of skeletal muscle autophagy and integrity, Nat. Commun. 14 (1) (2023) 1199.
[25] A. Franco-Romero, J.P. Leduc-Gaudet, S.N. Hussain, G. Gouspillou, M. Sandri, PHAF1/MYTHO is a novel autophagy regulator that controls muscle integrity, Autophagy 20 (4) (2024) 965–967.
[26] S. Kaushik, A.C. Massey, N. Mizushima, A.M. Cuervo, Constitutive activation of chaperone-mediated autophagy in cells with impaired macroautophagy, Mol. Biol. Cell 19 (5) (2008) 2179–2192.
[27] J.L. Schneider, Y. Suh, A.M. Cuervo, Deficient chaperone-mediated autophagy in liver leads to metabolic dysregulation, Cell Metabol. 20 (3) (2014) 417–432.
[28] A. Massey, S. Kaushik, G. Sovak, R. Kiffin, A. Cuervo, Consequences of the selective blockage of chaperone-mediated autophagy, Proc. Natl. Acad. Sci. USA 103 (15) (2006) 5805–5810.
[29] R. Kiffin, C. Christian, E. Knecht, A.M. Cuervo, Activation of chaperone-mediated autophagy during oxidative stress, Mol. Biol. Cell 15 (11) (2004) 4829–4840.
[30] M.E. Hubbi, H. Hu, Ahmed I. Kshitiz, A. Levchenko, G.L. Semenza, Chaperone-mediated autophagy targets hypoxia-inducible factor-1alpha (HIF-1alpha) for lysosomal degradation, J. Biol. Chem. 288 (15) (2013) 10703–10714.
[31] A. Gallego-Selles, M. Martin-Rincon, M. Martinez-Canton, M. Perez-Valera, S. Martín-Rodríguez, M. Gelabert-Rebato, et al., Regulation of Nrf2/Keap1 signalling in human skeletal muscle during exercise to exhaustion in normoxia, severe acute hypoxia and post-exercise ischaemia: influence of metabolite accumulation and oxygenation, Redox Biol. 36 (2020) 101627.
[32] R. Torres-Peralta, J. Losa-Reyna, M. Gonzalez-Izal, I. Perez-Suarez, J. Calle-Herrero, M. Izquierdo, J.A. Calbet, Muscle activation during exercise in severe acute hypoxia: role of absolute and relative intensity, High Alt. Med. Biol. 15 (4) (2014) 472–482.
[33] J.A. Calbet, J. Losa-Reyna, R. Torres-Peralta, P. Rasmussen, J.G. Ponce-González, A.W. Sheel, et al., Limitations to oxygen transport and utilization during sprint exercise in humans: evidence for a functional reserve in muscle O_2 diffusing capacity, J. Physiol. 593 (20) (2015) 4649–4664.
[34] D. Curtelin, D. Morales-Alamo, R. Torres-Peralta, P. Rasmussen, M. Martin-Rincon, M. Perez-Valera, et al., Cerebral blood flow, frontal lobe oxygenation and intra-arterial blood pressure during sprint exercise in normoxia and severe acute hypoxia in humans, J. Cerebr. Blood Flow Metabol. 38 (1) (2018) 136–150.
[35] D. Morales-Alamo, J. Losa-Reyna, R. Torres-Peralta, M. Martin-Rincon, M. Perez-Valera, D. Curtelin, et al., What limits performance during whole-body incremental exercise to exhaustion in humans? J. Physiol. 593 (20) (2015) 4631–4648.
[36] A. Gallego-Selles, V. Galvan-Alvarez, M. Martinez-Canton, E. Garcia-Gonzalez, D. Morales-Alamo, A. Santana, et al., Fast regulation of the NF-kappaB signalling pathway in human skeletal muscle revealed by high-intensity exercise and ischaemia at exhaustion: role of oxygenation and metabolite accumulation, Redox Biol. 55 (2022) 102398.
[37] M. Martin-Rincon, J.J. Gonzalez-Henriquez, J. Losa-Reyna, I. Perez-Suarez, J. G. Ponce-Gonzalez, J. de La Calle-Herrero, et al., Impact of data averaging strategies on VO_2max assessment: mathematical modeling and reliability, Scand. J. Med. Sci. Sports 29 (10) (2019) 1473–1488.
[38] B. Guerra, M.C. Gomez-Cabrera, J.G. Ponce-Gonzalez, V.E. Martinez-Bello, A. Guadalupe-Grau, A. Santana, et al., Repeated muscle biopsies through a single skin incision do not elicit muscle signaling, but IL-6 mRNA and STAT3 phosphorylation increase in injured muscle, J. Appl. Physiol. 110 (6) (2011) 1708–1715.
[39] B.A. Neel, Y. Lin, J.E. Pessin, Skeletal muscle autophagy: a new metabolic regulator, Trends Endocrinol. Metabol. 24 (12) (2013) 635–643.
[40] R.C. Russell, Y. Tian, H. Yuan, H.W. Park, Y.Y. Chang, J. Kim, et al., ULK1 induces autophagy by phosphorylating Beclin-1 and activating VPS34 lipid kinase, Nat. Cell Biol. 15 (7) (2013) 741–750.
[41] N. Mizushima, T. Yoshimori, How to interpret LC3 immunoblotting, Autophagy 3 (6) (2007) 542–545.
[42] Y. Katsuragi, Y. Ichimura, M. Komatsu, p62/SQSTM1 functions as a signaling hub and an autophagy adaptor, FEBS J. 282 (24) (2015) 4672–4678.
[43] G. Bjørkøy, T. Lamark, S. Pankiv, A. Øvervatn, A. Brech, T. Johansen, Monitoring autophagic degradation of p62/SQSTM1, Methods Enzymol. 452 (2009) 181–197.
[44] Y. Ichimura, S. Waguri, Y.S. Sou, S. Kageyama, J. Hasegawa, R. Ishimura, et al., Phosphorylation of p62 activates the Keap1-Nrf2 pathway during selective autophagy, Mol. Cell 51 (5) (2013) 618–631.
[45] F. Broering, Mytho: an Uncharacterized Foxo-dependent Gene that Controls Autophagy and Skeletal Muscle Mass, Master of Science Doctoral Dissertation, McGill University, Quebec, Canada, 2022.
[46] A.M. Cuervo, J.F. Dice, A receptor for the selective uptake and degradation of proteins by lysosomes, Science 273 (5274) (1996) 501–503.
[47] M. Pajares, A.I. Rojo, E. Arias, A. Diaz-Carretero, A.M. Cuervo, A. Cuadrado, Transcription factor NFE2L2/NRF2 modulates chaperone-mediated autophagy through the regulation of LAMP2A, Autophagy 14 (8) (2018) 1310–1322.
[48] A.M. Cuervo, E. Wong, Chaperone-mediated autophagy: roles in disease and aging, Cell Res. 24 (1) (2014) 92–104.
[49] F.A. Agarraberes, S.R. Terlecky, J.F. Dice, An intralysosomal hsp70 is required for a selective pathway of lysosomal protein degradation, J. Cell Biol. 137 (4) (1997) 825–834.
[50] D. Morales-Alamo, J.G. Ponce-Gonzalez, A. Guadalupe-Grau, L. Rodriguez-Garcia, A. Santana, M.R. Cusso, et al., Increased oxidative stress and anaerobic energy release, but blunted Thr^{172}-AMPKalpha phosphorylation, in response to sprint exercise in severe acute hypoxia in humans, J. Appl. Physiol. 113 (6) (2012) 917–928.
[51] W.G. Kaelin Jr., P.J. Ratcliffe, Oxygen sensing by metazoans: the central role of the HIF hydroxylase pathway, Mol. Cell 30 (4) (2008) 393–402.
[52] F.B. Favier, F.A. Britto, D.G. Freyssenet, X.A. Bigard, H. Benoit, HIF-1-driven skeletal muscle adaptations to chronic hypoxia: molecular insights into muscle physiology, Cell. Mol. Life Sci. 72 (24) (2015) 4681–4696.
[53] H. Ameln, T. Gustafsson, C.J. Sundberg, K. Okamoto, E. Jansson, L. Poellinger, Y. Makino, Physiological activation of hypoxia inducible factor-1 in human skeletal muscle, Faseb. J. 19 (8) (2005) 1009–1011.
[54] C.E.J. Moore, H. Mikolajek, S. Regufe Da Mota, X. Wang, J.W. Kenney, J. M. Werner, C.G. Proud, Elongation factor 2 kinase is regulated by proline hydroxylation and protects cells during hypoxia, Mol. Cell Biol. 35 (10) (2015) 1788–1804.
[55] D.M. Gwinn, D.B. Shackelford, D.F. Egan, M.M. Mihaylova, A. Mery, D.S. Vasquez, et al., AMPK phosphorylation of raptor mediates a metabolic checkpoint, Mol. Cell 30 (2) (2008) 214–226.
[56] N. Hosokawa, T. Hara, T. Kaizuka, C. Kishi, A. Takamura, Y. Miura, et al., Nutrient-dependent mTORC1 association with the ULK1-Atg13-FIP200 complex required for autophagy, Mol. Biol. Cell 20 (7) (2009) 1981–1991.

[57] C. Mammucari, G. Milan, V. Romanello, E. Masiero, R. Rudolf, P. Del Piccolo, et al., FoxO3 controls autophagy in skeletal muscle in vivo, Cell Metabol. 6 (6) (2007) 458–471.
[58] N. Mizushima, A. Yamamoto, M. Matsui, T. Yoshimori, Y. Ohsumi, In vivo analysis of autophagy in response to nutrient starvation using transgenic mice expressing a fluorescent autophagosome marker, Mol. Biol. Cell 15 (3) (2004) 1101–1111.
[59] J.W. Kenney, C.E. Moore, X. Wang, C.G. Proud, Eukaryotic elongation factor 2 kinase, an unusual enzyme with multiple roles, Adv Biol Regul 55 (2014) 15–27.
[60] G.J. Browne, S.G. Finn, C.G. Proud, Stimulation of the AMP-activated protein kinase leads to activation of eukaryotic elongation factor 2 kinase and to its phosphorylation at a novel site, serine 398, J. Biol. Chem. 279 (13) (2004) 12220–12231.
[61] S.B.G. Horman, U. Krause, J. Patel, D. Vertommen, L. Bertrand, A. Lavoinne, L. Hue, C. Proud, M. Rider, Activation of AMP-activated protein kinase leads to the phosphorylation of elongation factor 2 and an inhibition of protein synthesis, Curr. Biol. 12 (16) (2002) 1419–1423.
[62] X. Wang, S. Regufe da Mota, R. Liu, C.E. Moore, J. Xie, F. Lanucara, et al., Eukaryotic elongation factor 2 kinase activity is controlled by multiple inputs from oncogenic signaling, Mol. Cell Biol. 34 (22) (2014) 4088–4103.
[63] T. Akimoto, S.C. Pohnert, P. Li, M. Zhang, C. Gumbs, P.B. Rosenberg, et al., Exercise stimulates Pgc-1alpha transcription in skeletal muscle through activation of the p38 MAPK pathway, J. Biol. Chem. 280 (20) (2005) 19587–19593.
[64] A. Vainshtein, L.D. Tryon, M. Pauly, D.A. Hood, Role of PGC-1α during acute exercise-induced autophagy and mitophagy in skeletal muscle, Am. J. Physiol. Cell Physiol. 308 (9) (2015) C710–C719.
[65] A. Saleem, D.A. Hood, Acute exercise induces tumour suppressor protein p53 translocation to the mitochondria and promotes a p53-Tfam-mitochondrial DNA complex in skeletal muscle, J. Physiol. 591 (14) (2013) 3625–3636.
[66] K. Baar, A.R. Wende, T.E. Jones, M. Marison, L.A. Nolte, M. Chen, et al., Adaptations of skeletal muscle to exercise: rapid increase in the transcriptional coactivator PGC-1, Faseb. J. 16 (14) (2002) 1879–1886.
[67] Z. Yan, V.A. Lira, N.P. Greene, Exercise training-induced regulation of mitochondrial quality, Exerc. Sport Sci. Rev. 40 (3) (2012) 159–164.
[68] I. Scott, B.R. Webster, C.K. Chan, J.U. Okonkwo, K. Han, M.N. Sack, GCN5-like protein 1 (GCN5L1) controls mitochondrial content through coordinated regulation of mitochondrial biogenesis and mitophagy, J. Biol. Chem. 289 (5) (2014) 2864–2872.
[69] S. Takikita, C. Schreiner, R. Baum, T. Xie, E. Ralston, P.H. Plotz, N. Raben, Fiber type conversion by PGC-1α activates lysosomal and autophagosomal biogenesis in both unaffected and Pompe skeletal muscle, PLoS One 5 (12) (2010) e15239.
[70] T. Tsunemi, T.D. Ashe, B.E. Morrison, K.R. Soriano, J. Au, R.A. Roque, et al., PGC-1α rescues Huntington's disease proteotoxicity by preventing oxidative stress and promoting TFEB function, Sci. Transl. Med. 4 (142) (2012) 142ra97.
[71] D.A. Hood, G. Uguccioni, A. Vainshtein, D. D'Souza, Mechanisms of exercise-induced mitochondrial biogenesis in skeletal muscle: implications for health and disease, Compr. Physiol. 1 (3) (2011) 1119–1134.
[72] S. Jäger, C. Handschin, J. St-Pierre, B.M. Spiegelman, AMP-activated protein kinase (AMPK) action in skeletal muscle via direct phosphorylation of PGC-1alpha, Proc. Natl. Acad. Sci. U. S. A. 104 (29) (2007) 12017–12022.
[73] J.P. Little, A. Safdar, D. Bishop, M.A. Tarnopolsky, M.J. Gibala, An acute bout of high-intensity interval training increases the nuclear abundance of PGC-1α and activates mitochondrial biogenesis in human skeletal muscle, Am. J. Physiol. Regul. Integr. Comp. Physiol. 300 (6) (2011) R1303–R1310.
[74] J.A.L. Calbet, S. Martín-Rodríguez, M. Martin-Rincon, D. Morales-Alamo, An integrative approach to the regulation of mitochondrial respiration during exercise: focus on high-intensity exercise, Redox Biol. 35 (2020).
[75] D. Morales-Alamo, J.A.L. Calbet, AMPK signaling in skeletal muscle during exercise: role of reactive oxygen and nitrogen species, Free Radic. Biol. Med. 98 (2016) 68–77.
[76] N.K. Tonks, Protein tyrosine phosphatases: from genes, to function, to disease, Nat. Rev. Mol. Cell Biol. 7 (11) (2006) 833–846.
[77] S.E. Wohlgemuth, A.Y. Seo, E. Marzetti, H.A. Lees, C. Leeuwenburgh, Skeletal muscle autophagy and apoptosis during aging: effects of calorie restriction and life-long exercise, Exp. Gerontol. 45 (2) (2010) 138–148.
[78] M. Komatsu, S. Waguri, M. Koike, Y.S. Sou, T. Ueno, T. Hara, et al., Homeostatic levels of p62 control cytoplasmic inclusion body formation in autophagy-deficient mice, Cell 131 (6) (2007) 1149–1163.
[79] P. Leurcharusmee, P. Sawaddiruk, Y. Punjasawadwong, N. Sugandhavesa, K. Klunklin, S. Tongprasert, et al., Ischemic preconditioning upregulates Mitofusin2 and preserves muscle strength in tourniquet-induced ischemia/reperfusion, J Orthop Translat 35 (2022) 113–121.
[80] A.N. Bailey, A.D. Hocker, B.R. Vermillion, K. Smolkowski, S.N. Shah, B.A. Jewett, H.C. Dreyer, MAFbx, MuRF1, and the stress-activated protein kinases are upregulated in muscle cells during total knee arthroplasty, Am. J. Physiol. Regul. Integr. Comp. Physiol. 303 (4) (2012) R376–R386.
[81] B. Shadgan, W.D. Reid, R.L. Harris, S. Jafari, S.K. Powers, P.J. O'Brien, Hemodynamic and oxidative mechanisms of tourniquet-induced muscle injury: near-infrared spectroscopy for the orthopedics setting, J. Biomed. Opt. 17 (8) (2012), 081408-1.
[82] W.A. Meier, R.L. Marcus, L.E. Dibble, K.B. Foreman, C.L. Peters, R.L. Mizner, P. C. LaStayo, The long-term contribution of muscle activation and muscle size to quadriceps weakness following total knee arthroplasty, J. Geriatr. Phys. Ther. 32 (2) (2009) 79–82.
[83] M. Sandri, Autophagy in skeletal muscle, FEBS (Fed. Eur. Biochem. Soc.) Lett. 584 (7) (2010) 1411–1416.
[84] E. Barbieri, P. Sestili, Reactive oxygen species in skeletal muscle signaling, J Signal Transduct 2012 (1) (2012) 982794.
[85] A.I. Alayash, R.P. Patel, R.E. Cashon, Redox reactions of hemoglobin and myoglobin: biological and toxicological implications, Antioxidants Redox Signal. 3 (2) (2001) 313–327.
[86] I. Irrcher, V. Ljubicic, D.A. Hood, Interactions between ROS and AMP kinase activity in the regulation of PGC-1α transcription in skeletal muscle cells, Am. J. Physiol. Cell Physiol. 296 (1) (2009) C116–C123.
[87] M. Rahman, M. Mofarrahi, A.S. Kristof, B. Nkengfac, S. Harel, S.N.A. Hussain, Reactive oxygen species regulation of autophagy in skeletal muscles, Antioxidants Redox Signal. 20 (3) (2013) 443–459.
[88] R. Scherz-Shouval, E. Shvets, E. Fass, H. Shorer, L. Gil, Z. Elazar, Reactive oxygen species are essential for autophagy and specifically regulate the activity of Atg4, EMBO J. 26 (7) (2007) 1749–1760.
[89] E.E. Talbert, A.J. Smuder, K. Min, O.S. Kwon, H.H. Szeto, S.K. Powers, Immobilization-induced activation of key proteolytic systems in skeletal muscles is prevented by a mitochondria-targeted antioxidant, J. Appl. Physiol. 115 (4) (2013) 529–538.
[90] M.A. Essers, S. Weijzen, A.M. de Vries-Smits, I. Saarloos, N.D. de Ruiter, J.L. Bos, B. M. Burgering, FOXO transcription factor activation by oxidative stress mediated by the small GTPase Ral and JNK, EMBO J. 23 (24) (2004) 4802–4812.
[91] K. Chen, P. Gao, Z. Li, A. Dai, M. Yang, S. Chen, et al., Forkhead box O signaling pathway in skeletal muscle atrophy, Am. J. Pathol. 192 (12) (2022) 1648–1657.
[92] A. Puissant, N. Fenouille, P. Auberger, When autophagy meets cancer through p62/SQSTM1, Am. J. Cancer Res. 2 (4) (2012) 397–413.
[93] K.B. Larsen, T. Lamark, A. Øvervatn, I. Harneshaug, T. Johansen, G. Bjørkøy, A reporter cell system to monitor autophagy based on p62/SQSTM1, Autophagy 6 (6) (2010) 784–793.
[94] M Pajares, AI Rojo, E Arias, A Diaz-Carretero, AM Cuervo, A Cuadrado, Transcription factor NFE2L2/NRF2 modulates chaperone-mediated autophagy through the regulation of LAMP2A, Autophagy 14 (8) (2018) 1310–1322.